Published in *Solar Energy 176, pp. 194-210, 2018*
DOI: *10.1016/j.solener.2018.10.003*

An inverse approach to identify selective angular properties of retro-reflective materials for Urban Heat Island mitigation

Mattia Manni[a], Gabriele Lobaccaro[b,#], Francesco Goia[b,#,*], Andrea Nicolini[a,c]

[a] *CIRIAF – Interuniversity Research Center on Pollution and Environment "Mauro Felli", Perugia, Italy.*

[b] *Department of Architecture and Technology, Faculty of Architecture and Design, Norwegian University of Science and Technology NTNU, Trondheim, Norway.*

[c] *Department of Engineering, University of Perugia, Perugia, Italy*

[#] *Member of ISES® - International Solar Energy Society®*

[*]*Corresponding author. Tel.: +47 450 274 37. E-mail address: francesco.goia@ntnu.no (F. Goia).*

Abstract

This work presents the preliminary stages of a wider study aiming at assessing the potentials of retro-reflective (RR) materials to mitigate urban heat island effects. Th study herewith reported is based on an inverse approach, which originates from the evaluation of the solar irradiation incident on urban surfaces (i.e. façade, roof, and paving) and leads to the identification of the optimal angular properties required to activate such a material. The solar radiation geometry and the solar irradiation collected by the south-exposed vertical and the horizontal surfaces, were assessed by solar dynamic simulation tools. Furthermore, the angular distribution of the solar direct irradiation component and the direct to global solar irradiation ratio were estimated. The analyses were carried out for nine locations between Oulu (Finland) and Doha (Qatar), with an increment of 5° latitude between two locations.

The results demonstrate that the application of RR materials to horizontal surfaces can always be effective, whereas when applied on the vertical surface, the solar geometry influences to a much greater extent the performance of these materials. The main findings of this study show that the selective angular properties of an ideal RR material should be in the angular interval between 25° and 55° and between 30° and 90°, in case of vertical surfaces and horizontal surfaces, respectively. Best practices related to the application of RR materials and the activation of their selective angular properties in different climate zones are also reported.

Keywords: retro-reflective materials, selective angular properties, solar irradiation, urban heat island.

Published in *Solar Energy 176, pp. 194-210, 2018*
DOI: *10.1016/j.solener.2018.10.003*

1. Introduction

The risk of Urban Heat Islands (UHI) is increasing with the spread of urban areas (United Nations, 2014; Brans et al., 2018; Lin et al., 2018) and climate change (Han et al., 2015). This implies that the temperature in cities can be far higher than in rural surroundings because of the extra energy requirements for cooling and guaranteeing an adequate level of human thermal comfort (Pantavou et al., 2011). Exposing built surfaces with certain finishing to direct solar radiation leads to an increment of both the surface and the atmosphere's temperature, with an impact on local weather conditions, building energy use (Santamouris et al., 2007), and comfort conditions of the inhabitants (Radhi et al., 2015). Furthermore, the overwarming of the urban areas could also impact on canyon ventilation and pollutant dispersion (Stathopoulou et al., 2008), which are important factors for people's health and air quality (Santamouris and Kolokotsa, 2015).

Several studies focused on the development of technologies and strategies, which can mitigate the UHI effect. Among these, it is worth mentioning: high albedo surfaces (i.e. cool materials), green areas, and heat storage systems (e.g. phase change materials). Evidences from different research activities has proven that these solutions can reduce the outdoor air temperature by up to 5 °C (Radhi et al., 2015) in urbanized areas, with a consequent lowering of the energy requirements for cooling (Xu et al., 2018). Different investigations (Hassid et al., 2000, Santamouris, 2014, Santamouris et al., 2015) have revealed that the estimation of energy use in buildings cannot be reliably conducted without considering the UHI effect on buildings and have demonstrated that the average increase of the cooling demand is around 23%, whereas the corresponding average reduction of the heating demand is around 19%. In total, the average energy demand of building appears to increase by more than 10% when including UHI-related thermal loads (Santamouris et al., 2015).

In this context, this work presents the first part of a wider study that aims at mitigating overwarming effect through the adoption of retro-reflective (RR) materials characterized by selective properties, with consideration of to the different climates where they can be applied. The RR materials partially redirected back towards the sky the incoming solar radiation and contribute to reduce the urban temperature in the urban setting.

The paper is organized according to the following sections: a background, where a brief state of the art, knowledge gap, and aim of the activity are presented; a methodology section, where the research approach, workflow, model, tools, and data post-processing, as well as, the case-study locations are illustrated; a result and discussion chapter, where the outcomes of the research activities are presented for three different climatic areas, and the limitations of the study are highlighted. A chapter regarding best practices for selective properties of RR materials in different zones is then presented, followed by a conclusion section where an outlook of the further developments in the research activity is given.

Nomenclature table

RR	retro-reflective
UHI	urban heat island

Published in *Solar Energy 176, pp. 194-210, 2018*
DOI: *10.1016/j.solener.2018.10.003*

Irr_{dir}	direct solar irradiation
Irr_{dir}/Irr_{gl}	direct to global solar irradiation ratio
Irr_{gl}	global solar irradiation
Irr_{dif}	diffuse solar irradiation
ab	ambient bounces

2. Background

2.1. State of the art and current knowledge on retro-reflective materials

RR materials are engineered surfaces or surface treatments that can reflect incident solar radiation back towards the sky, and thus reduce mutual radiative effect among surfaces in close proximity. Their application as new urban materials is meant to (i) reduce the energy loads in the UHI boundary, (ii) reflect the solar radiation beyond the urban canyon, and (iii) decrease the mutual inter-buildings solar reflections. In this section, an overview of the state of the art (Table 1) of the development of RR materials and their applications is presented.

Despite RR materials having been widely employed for decades as street signs or targeting systems, only recently their application in the building sector has been explored. The studies conducted by Nielsen and Lu (Nilsen and Lu, 2004) describe the technology and parameters of the RR materials and propose, among other applications, the use of RR materials in buildings. RR materials are a subgroup of high-reflective layers (i.e. cool materials), and have proven to be a valid and efficient alternative to the traditional building's materials. In the review article conducted by Yuan et al. (2016), it was demonstrated that RR materials can guarantee a higher efficiency than high-reflective materials. Nevertheless, the lack of performance standards represents the main barrier for the application of RR materials. During the last decade, several research activities (Sakai et al., 2012, Rossi et al., 2014, Akbari and Touchaei, 2014, Rossi et al., 2015, Qin et al., 2016) have focused on the characterization of RR materials, ranging from the definition of an assessing protocol to the evaluation of RR properties. Commercial films, made of prism-array structures, capsule-lens, and bead-embedded layers, were analyzed and compared after they have been tested to miniature models of urban canyons or districts, to demonstrate their effectiveness in mitigating UHI (Sakai et al., 2012; Pisello et al., 2013). The benefits of the application of RR materials, such as the reduction of the surface temperature and the increment of the urban albedo, were investigated by Akbari and Touchaei (2014), and Rossi et al. (2015). Their investigations led to the definition of two analytical models, validated using urban canyon prototypes. Other research activities reveled that a reduction of energy demand up to 10% can be achieved by adopting RR façades in place of traditional cool materials (Han et al., 2015). The analysis of the performance of RR materials was also carried out experimentally. The efficiency of RR materials was tested with a measurement facility equipped with 19 photodiodes to estimate the reflected fractions in different directions.

In particular, these tests aimed at studying materials characterized by the largest possible angular range of retro-reflection. Indeed, a retro-reflected behavior can be usually observed when the solar irradiation hits the RR material mainly perpendicularly, while a high-reflective behavior is shown in case of mostly parallel sunrays' direction (Rossi et al., 2015).

The application of RR layers was also analyzed on both opaque and transparent surface, and in the latter case in combination with glazed surfaces. Yoshida et al. (2015) studied a single glass pane window enhanced with heat ray RR films, showing how the peak of the mean radiant temperature is reduced by up to more than 4 °C in comparison with a low-E double glass window. Similarly, Ichinose et al. (2017) found that low-E glass performs better in terms of energy consumption, but they reflect a higher quantity of direct irradiation (Irrdir) toward the urban canopy compared to the RR application – and this in turn, increases the upward reflection factor averagely by 5% (Inoue et al., 2017).

Despite of the proven advantages of the different RR technologies, there are still some aspects that need to be addressed to enable this systems to reach their full potentials. Among these, it is worth mentioning the increased light pollution and the decreased solar loads in winter. As a matter of fact, the RR materials could present some side effects such as (i) the increment of heating energy requirements in winter, since less solar energy is absorbed by the façades; and (ii) the higher lighting pollution level due to the reduction of urban surfaces able to absorb the city lights. To overcome these potential issues, two materials have been proposed by Sakai and Iyota (2017), and can be classified as selective RR materials. The first is a RR layer characterized by a pattern depending on the latitude. From the yearly analysis of the focal points of the sunlight, a "high-spec directional-type" coating was developed for absorbing solar radiation in winter while reducing cooling loads in summer. The second one is inspired by the moon's RR behavior. It is defined as a "rough-surface-type" RR material and its retro-reflectivity is due to the combination of its surface roughness and its diffuse reflection.

The development of RR materials underlines two main tendencies: on one hand, durable RR materials characterized by the best performance level in terms of retro-reflection, without considering any other parameters, are searched (Yuan et al., 2014, Yuan et al., 2015a, 2015Yuan et al., 2015b, Yuan et al., 2016a, Yuan et al., 2016b). On other hand, the chromatic alteration that the RR material can generate if applied on existing – or even historical – buildings (Cotana et al., 2015, Rossi et al., 2015, Rossi et al., 2016, Castellani et al., 2017, Morini et al., 2017b, Morini et al., 2017b, Morini et al., 2018) is investigated. These two different trends led to the development of two classes of RR materials with different performance levels. The two RR materials have also been exposed to a degradation which is almost 100% reversible (Yuan et al., 2015a, Yuan et al., 2015b) and their application can increase the urban canyon's albedo by around 7% (Morini et al., 2017a).

2.2. Knowledge-gap and aim of the research activity

So far, the development of RR materials has primarily focused on enhancing the materials' performance, with limited consideration of the context-related variables, except in Sakai and Iyota (2017).

Year	Location	Application			Calculated parameters								Models			Reference
		Window	Opaque surface	Paving / Roofing	Impact on Urban canyon	Heat flow	Cooling demand	Global reflectance	RR properties	Color modification	Durability *[month]*	Carbon emissions	Analytical	Prototype	Digital model	
2004	N/A	-	✓	-	-	-	-	✓	✓	-	-	-	-	-	-	(Sakai, Emura and Igawa, 2008)
2012	Japan	-	✓	✓	✓	-	-	✓	✓	-	-	-	-	✓	-	(Sakai, Emura and Igawa, 2008)
2014	Italy	-	✓	-	✓	-	-	✓	✓	-	-	-	✓	✓	-	(Pisello *et al.*, 2013)
	N/A	-	-	✓	-	✓	✓	✓	-	-	-	-	✓	-	✓	(Akbari and Touchaei, 2014)
	Japan	✓	-	-	✓	✓	✓	-	✓	-	-	-	✓	-	-	(Yoshida *et al.*, 2015)
2015	Italy	-	✓	-	✓	-	-	✓	✓	✓	-	-	-	✓	✓	(Rossi *et al.*, 2015)
2015	Italy	-	✓	-	✓	-	-	✓	-	-	-	-	-	✓	-	(Cotana, 2015)
	Japan	-	✓	-	-	✓	-	✓	✓	-	-	-	✓	✓	✓	(Jihui Yuan, Farnham and Emura, 2015)
	United States of America	-	✓	-	✓	✓	✓	✓	-	-	-	-	-	-	✓	(Han, Taylor and Pisello, 2015)
	Japan	-	✓	-	-	✓	-	✓	✓	-	25	-	✓	✓	-	(Yuan, Emura and Farnham, 2014)
	Japan	-	✓	-	✓	✓	✓	✓	✓	-	16	✓	✓	✓	✓	(J. Yuan, Farnham and Emura, 2015)
2016	Italy	-	-	✓	✓	-	-	✓	✓	-	-	-	✓	✓	-	(Rossi *et al.*, 2016)
	Japan	-	✓	-	✓	✓	✓	✓	✓	-	-	-	✓	✓	✓	(Yuan, Emura, Farnham, *et al.*, 2016)
	Japan	-	✓	-	-	✓	-	✓	✓	-	-	-	✓	✓	-	(Yuan, Emura, Sakai, *et al.*, 2016)
	N/A	-	✓	-	✓	✓	✓	✓	✓	-	-	-	-	-	-	(Yuan, Emura and Farnham, 2016)
	China	-	✓	-	✓	-	-	✓	✓	-	-	-	-	✓	-	(Qin *et al.*, 2016)
2017	Italy	-	✓	-	✓	-	-	✓	✓	✓	-	-	-	✓	✓	(Morini, Castellani, Presciutti, Filipponi, *et al.*, 2017)
	Italy	-	✓	-	✓	-	✓	✓	✓	-	-	-	✓	✓	-	(Morini, Castellani, Presciutti, Anderini, *et al.*, 2017)
	Japan	✓	-	-	✓	✓	✓	✓	✓	-	-	-	-	✓	✓	(Ichinose, Inoue and Nagahama, 2017)
	Japan	-	✓	✓	-	-	-	✓	✓	-	-	-	-	✓	-	(Sakai and Iyota, 2017)
	Italy	-	✓	-	-	-	-	✓	✓	✓	-	-	✓	✓	-	(Castellani *et al.*, 2017)
	Japan	✓	-	-									-	✓	✓	(Inoue *et al.*, 2017)
2018	Italy	-	✓	-	-	-	-	✓	✓	✓	-	-	✓	✓	-	(Morini *et al.*, 2018)

Table 1 Tabular review of the state-of-the-art regarding RR technology and possible applications.

Most of the research and development was oriented towards the increment of the angular range of activation of RR behavior, and only recently, the possible selective behavior of RR materials has been investigated. Until now, the amount of available solar irradiation that hits the surface in that range of retro-reflection has been only marginally explored. The lack of preliminary solar analyses for RR material development, as well as, the lack of knowledge on the maximum achievable efficiency by applying RR technology, represent two barriers in the development of RR materials and their application on urban surfaces (i.e. façade, roof, and paving). The methodology proposed in this work is a first attempt to cover these gaps: it moves from the environmental assessment towards the identification of an ideal RR material characterized by a selective behavior. Thus, the main domain of research covers (a) the reliability of the solar-oriented approach to the enhancement of RR materials, (b) the suitability of the seasonal angular distribution of Irrdir to be exploited for developing a selective behavior of RR materials, and (c) the effectiveness of RR technology and its application at different latitudes.

Published in *Solar Energy 176, pp. 194-210, 2018*
DOI: *10.1016/j.solener.2018.10.003*

3. Methodology

The study of the properties of RR material is usually carried out by straightforward approaches, which focus on increasing the angular range in which a RR behavior can be observed. This study follows instead an "inverse approach" and investigates the selective angular properties for RR materials that would enhance their performance by analyzing the solar irradiation on vertical and horizontal surface. It can be considered a reverse approach since it moves from the evaluation of the available solar energy towards the definition of the angular properties characterizing RR materials at different latitudes.

Therefore, this work aims at assessing the solar irradiation impinging on a given surface and its angular distribution – i.e. the angles of incidence that characterized the contributions of Irrdir collected by a surface – as well as, the seasonal direct to global solar irradiation ratio (Irrdir/Irrgl). The analysis is carried out in different locations, ranging from the Arctic to the Persian Gulf area. The comparison of the outcomes at different latitudes allows defining best practices for the application of RR materials in each specific climate zone.

3.1. Model, workflow, tools, and data post-processing

The overview of the three-stage workflow (data generation (stage a), data elaboration (stage b), and data assessment (stage c)) is illustrated in Fig. 1. The climatic data and the building's geometry are the inputs in stage a. The main outcomes of this stage are (i) the angles of incidence of sunrays and (ii) the hourly values of solar irradiation (global solar irradiation (Irrgl), Irrdir, and solar diffuse irradiation (Irrdif)) collected by the analyzed surface. The data elaboration, stage b, is focused on the definition of the solar angular distribution by coupling the two variables from the stage a. The polar diagrams and the calculation of the ratio Irrdir/Irrgl, are generated with information about the cloud coverage and compared among the different latitudes (stage c). In the polar diagrams, an angular value equals to zero corresponds to the direction normal to the analyzed vertical surface, whereas in case of horizontal surface the null value corresponds to the parallel vector. Starting from the angular distribution of the Irrdir, three angular ranges were considered to calculate the Irrdir distributed around the seasonal energy peaks: 10°, 40°, and 90°. The first angular range (5° before and 5° after the seasonal peak, making the angular range 10° wide) allows the single, most intense peak to be identified; the second (20° before and 20° after the seasonal peak, making the angular range 40° wide) corresponds to the angular range in which a retro-reflection behaviour can be observed with the existing materials; the third range (90°) corresponds to the totality of the solar angular distribution. The ratio Irrdir/Irrgl, allows assessing the seasonal amount of solar irradiation involved in the retro-reflection phenomenon, as this represents the percentage of the solar irradiation that can be reflected back towards the sky and therefore potentially not trapped in the urban canopies.

Published in *Solar Energy 176, pp. 194-210, 2018*
DOI: *10.1016/j.solener.2018.10.003*

The yearly solar irradiation analyses are organized according to the four seasons: spring (March, April, May), summer (June, July, August), fall (September, October, November), and winter (December, January, February). This approach allows assessing the potential of seasonal behavior (through selective RR materials). In the solar analyses, the cloud coverage value reported in the weather data file (based on the Typical Meteorological Year – TMY) was used. The TMY data contained in the EnergyPlus weather (.epw) files (energyplus.net/weather) were used in this study.

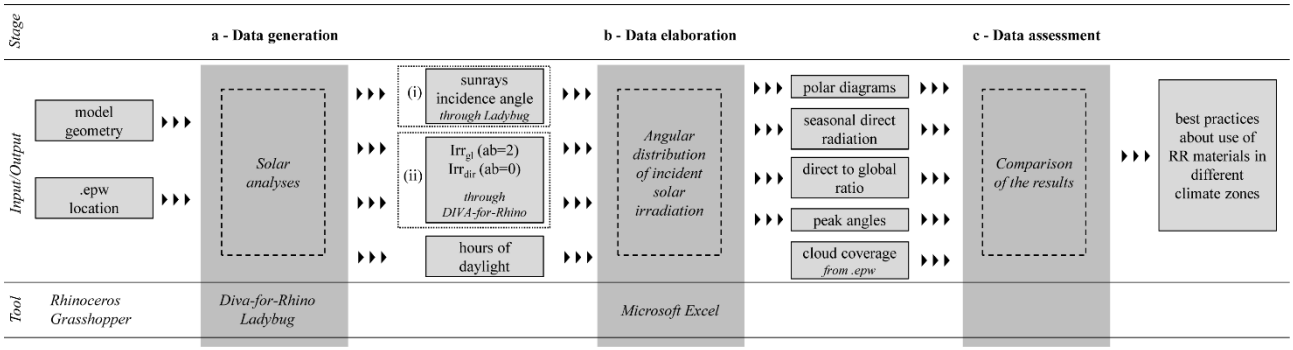

Figure 1 Overview of the workflow. The main inputs and outputs are reported for each stage along with the employed tools.

Solar irradiation analyses were conducted on both a vertical and a horizontal surface of a box-shape virtual building (a 10 m × 10 m × 10 m cube) placed in an unobstructed urban environment, with the four main elevations oriented towards the four main directions. The reason for this choice is that, in this first part of the research activity, the focus is placed on the maximal theoretical behavior of RR materials, which can be obtained in the case of unobstructed surfaces. As far as the horizontal surface is concerned, this means that the analysis carried out is valid for a RR material applied to either roofing or paving systems. As far as the vertical surfaces is concerned, the analyses presented in this paper are limited to the orientation, among the four main exposures of the building's facades, in which the highest Irrdir is measured (Table 2). As confirmed by some studies in literature (Ibrahim et al., 2014, Lobaccaro et al., 2018), in all analysed locations, the south-exposed façade is the one with the highest value of Irrdir. In the following sections of the papers, the terms "vertical surface" refers therefore to a south-exposed surface.

Table 2 Overview of the Irr_{dir} collected by building's façades at different latitudes.

Location		**Coordinates**		**Irr_{gl}** [kWh/m^2]			
City	**Country**	**Latitude**	**Longitude**	***East***	***South***	***West***	***North***
Oslo	Norway	59°57′ N	10°45′ E	450	720	440	205
Milan	Italy	45°28′ N	9°11′ E	585	870	590	250
Cairo	Egypt	30°03′ N	31°14′ E	815	995	815	310

The building block was modeled in the Grasshopper environment and visualized in the Rhinoceros environment, while the Ladybug plug-in, based on Radiance engines, was used to investigate the solar geometry and to conduct yearly solar irradiation analyses (Fig. 2). Ladybug evaluates the sun path of the chosen location based on the .epw file. DIVA-for-Rhino, a Radiance-based plug-in, was used to conduct grid-based solar analyses to calculate the solar irradiation collected by a surface (vertical and horizontal).

Published in *Solar Energy 176, pp. 194-210, 2018*
DOI: *10.1016/j.solener.2018.10.003*

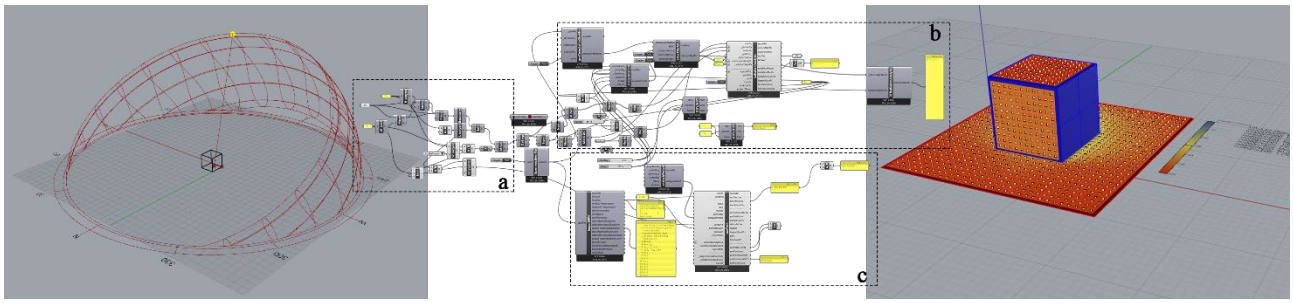

Figure 2 From the left: visualization of the model of building block and the sunray in *Rhinoceros* environment; the *Grasshopper* definition with the model part (a), the settings for solar irradiation simulation (b) and the calculation of the sun geometry and sun-angle (c); and the visualization of solar irradiation map on the vertical and horizontal surfaces.

The Radiance simulation parameters (Table 3) were set as follows: the value of ambient bounces (ab), that counts the number of the solar reflections before the sunray hits the analyzed surface, was set equal to two in order to estimate Irrgl; a null value was used to calculate the contribution of Irrdir. The grid of test points was generated at 0.1 m distance from the analyzed surfaces, and the cells' size was set to one meter by one meter.

Table 3 Set of 'rtrace' parameters employed for conducting solar radiation analyses with *Diva-for-Rhino*.

Ambient bounces	Ambient divisions	Ambient super samples	Ambient resolution	Ambient accuracy
0/2	1,000	20	300	0.1

Custom Radiance materials were defined for each surface (i.e. ground, façade, roof) (Table 4). The materials' properties were set considering the parameters of color (RGB values), specularity (fraction of incident light that is reflected; varying from 0.0 for a perfectly diffusive surface to 1.0 for a perfect mirror), and roughness (surface irregularities quantified by the deviation from its ideal direction of the normal vector of a real surface; the value varies from 0.0, which corresponds to a perfectly smooth surface, to 1.0 that corresponds to a perfectly irregular surface). In this study, the specularity, roughness and reflectance values of the ground surface (OutsideGround_00%R in Table 4) were set equal to zero to avoid the solar reflections from the ground. For vertical and horizontal surfaces, standard settings were given, considering that this preliminary study was focused on the analyses of Irrdir, Irrdif and Irrgl without considering the mutual inter-buildings solar reflections, and these settings do not affect the results.

Table 4 List of materials properties used in Radiance.

Surface	Radiance material	Materials / colors	Radiance material	Number of arguments	RGB reflectance	Effective reflectance values
Ground	OutsideGround_00%R	Asphalt	Void plastic	0 0 5	0.00	0.0
Vertical surface (Facades)	OutsideFaçade_30%R	Paint brown	Void plastic	0 0 5	0.30	0.22-0.36
Horizontal surface (Roof)	GenericCeiling_30%R	Grey concrete tiles	Void plastic	0 0 5	0.30	0.31–0.33

The analyses were conducted with an hourly time-step through the whole year. The irradiation quantities – expressed in kWh/m2 – were coupled to the corresponding angles of incidence of sunrays by an algorithm developed in a calculation sheet in Microsoft Office Excel. Furthermore, the ratio Irrdir/Irrgl was also considered to better evaluate potential impact of the RR materials – they can reflect towards the sky most of the direct component – while they do not interact with the

Published in *Solar Energy 176, pp. 194-210, 2018*
DOI: *10.1016/j.solener.2018.10.003*

diffuse solar irradiation component. An analysis of the cloud coverage index was also conducted in parallel to obtain a preliminary evaluation of effectiveness of the RR materials at different latitudes.

3.2. Case study cities

The case study locations were selected starting from the latitude of 25°N, with steps northward equal to 5° to cover heterogeneous climatic conditions in which the RR materials could be applied (Table 5). The locations were grouped in three clusters according to their latitude and climate: the Northern zone includes Oulu (Finland), Oslo (Norway) and Copenhagen (Denmark), the Central zone includes Brussels (Belgium), Milan (Italy) and Madrid (Spain), and the Southern zone includes Valletta (Malta), Cairo (Egypt) and Doha (Qatar).

Table 5 List of the case study cities: data are related to their locations and climate according to Köppen-Geiger model.

Zone	Country	City	Latitude	Longitude	Climate
Northern zone	*Finland*	Oulu	65°01′ N	25°28′ E	*Dfb*
	Norway	Oslo	59°57′ N	10°45′ E	*Dfb*
	Denmark	Copenhagen	55°41′ N	12°34′ E	*Cfb*
Central zone	*Belgium*	Brussels	50°51′ N	4°21′ E	*Cfb*
	Italy	Milan	45°28′ N	9°11′ E	*Cfa*
	Spain	Madrid	40°23′ N	3°43′ W	*Cfa*
Southern zone	*Malta*	Valletta	35°54′ N	14°31′ E	*Cfa*
	Egypt	Cairo	30°03′ N	31°14′ E	*BWh*
	Qatar	Doha	25°17′ N	51°32′ E	*BWh*

The zones are characterized by different climatic contexts, which range from extremely cold to subtropical or even desert. According to the Köppen-Geiger model (Kottek et al., 2006), in the Nordic zone (from latitude 65°N to latitude 55°N) the climate is classified as warm-summer humid continental climate (Oulu and Oslo) and temperate oceanic climate (Copenhagen). In the Central zone (from latitude 50°N to latitude 40°N), Brussels, Milan, and Madrid, are classified as temperate oceanic, humid sub-tropical, and Mediterranean hot-summer respectively. Finally, the Southern zone (from latitude 35°N to latitude 25°N) that includes the cities of Dubai, Cairo, and Valletta, is characterized by extreme warm climate conditions.

4. Results and discussion

4.1. Solar irradiation analyses on the vertical surface

4.1.1. Northern zone (Oulu, Oslo, Copenhagen)

The data of the Irrdir obtained from the yearly angular distribution (Fig. 3 and Table 6) underlines that the most significant contribution on the vertical surface in the Northern zone is presented in the spring and in the summer.

Published in *Solar Energy 176, pp. 194-210, 2018*
DOI: *10.1016/j.solener.2018.10.003*

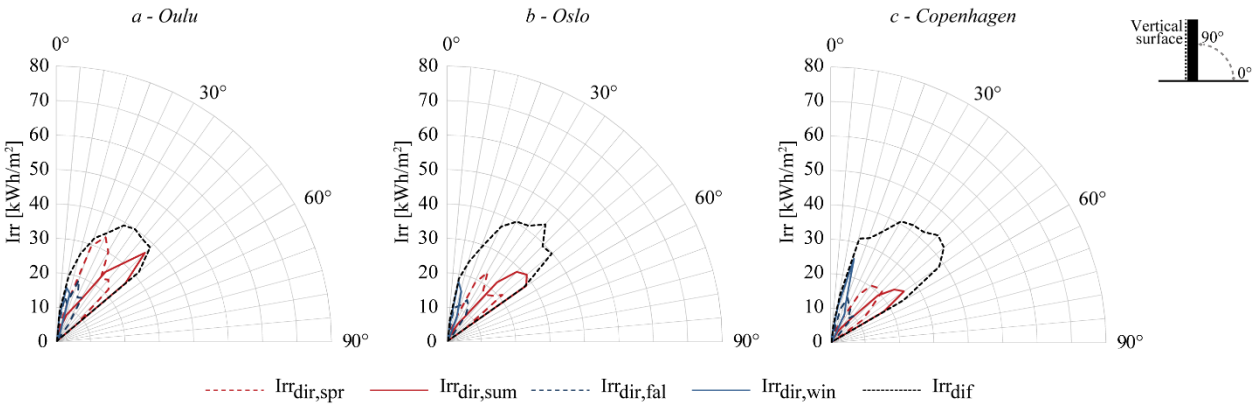

Figure 3 Yearly data of angular distribution of Irr_{dif} and Irr_{dir} on a vertical surface in the Northern zone. The Irr_{dir} data is presented in seasonal contributions.

Table 6 Summary of the yearly outcomes of number of hours of daylights, the Irr_{dir} and the Irr_{gl}. For each season are reported the highest value of the Irr_{dir} collected by the vertical surface considering an angular range of 10°, 40°, 90° respectively, the Irr_{gl} and the Irr_{dir}/Irr_{gl} ratio.

Case study cities	Number of hours of daylighting [h]	$Irr_{dir,yr}$ [kWh/m²]	$Irr_{gl,yr}$ [kWh/m²]	Season	Irr_{dir} 10° [kWh/m²]	Irr_{dir} 40° [kWh/m²]	Irr_{dir} 90° [kWh/m²]	Irr_{gl} [kWh/m²]	Irr_{dir}/Irr_{gl} [%]
Oulu	4,428	457	764	Spring	63	177	182	293	62
				Summer	65	152	153	287	53
				Fall	33	81	81	127	64
				Winter	30	40	40	55	72
Oslo	4,419	372	716	Spring	41	130	134	247	54
				Summer	58	124	124	270	46
				Fall	25	69	69	131	53
				Winter	32	44	44	67	66
Copenhagen	4,411	352	743	Spring	41	114	118	240	49
				Summer	49	105	105	263	40
				Fall	25	69	69	147	47
				Winter	37	59	59	92	64

During these seasons, in Oulu, the Irrdir is mainly concentrated in an azimuth angular range that varies from 10° to 50°, and the seasonal peaks are respectively registered at 25° in spring (33 kWh/m2), and 45° in summer (36 kWh/m2) (Fig. 4a). The amount of Irrdir collected by the vertical surface equals 182 kWh/m2 in spring and 153 kWh/m2 in summer (Table 6). They represent 63% of Irrgl in spring and 52% in summer. At this latitude, the highest value of Irrdir/Irrgl (72%) is reached in winter (Table 6), given that the sun angle is low from the horizon.

In Oslo, in spring and in summer, the solar irradiation is lower than in Oulu – in spring 134 kWh/m2 in Oslo and 182 kWh/m2 in Oulu and in summer 124 kWh/m2 in Oslo and 153 kWh/m2 in Oulu– because of the higher cloud coverage (Fig. 5). The cloud coverage also affects the ratio Irrdir/Irrgl in Oslo in spring and in summer that is equal to 54% and 46% respectively, while in winter it reaches the highest value in the Northern zone, up to 66% (Table 6).

Published in *Solar Energy 176, pp. 194-210, 2018*
DOI: *10.1016/j.solener.2018.10.003*

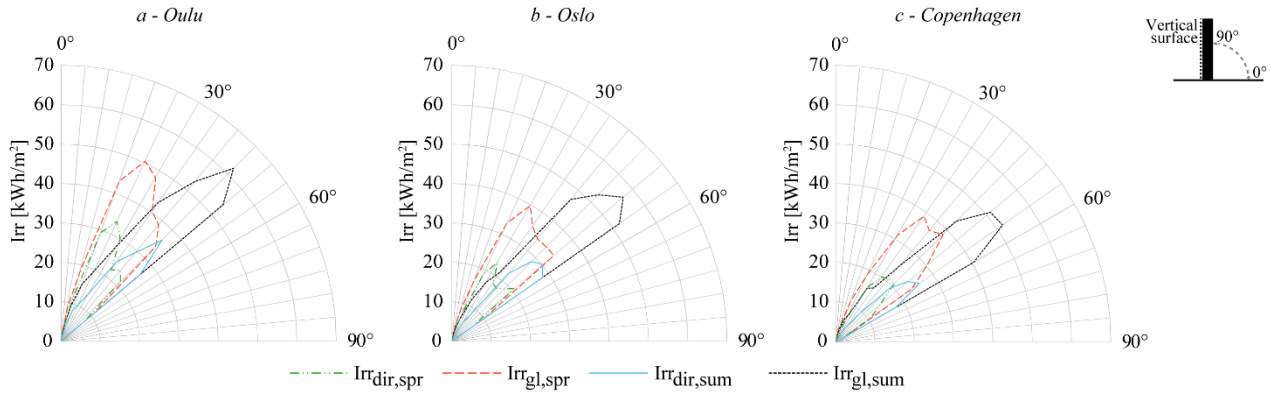

Figure 4 Angular distribution of Irrdir and Irrgl on the vertical surface in spring and in summer in the Northern zone.

In Copenhagen, the Irrdir/Irrgl ratios are the lowest of the Northern zone given the cloud coverage and the solar geometry: it equals 49% in spring and 40% in summer (Table 6).

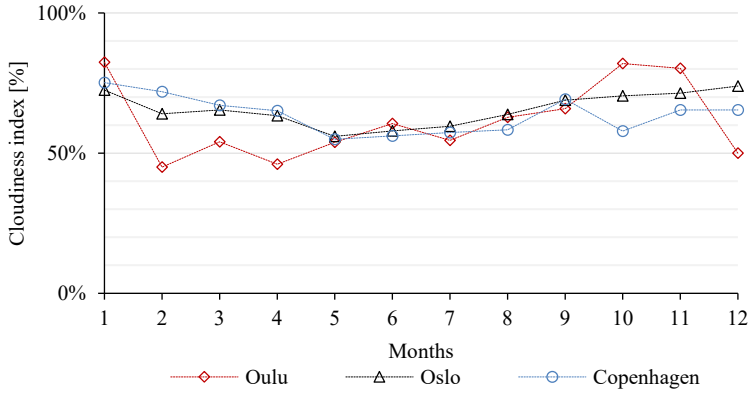

Figure 5 Monthly cloud coverage values calculated for each location of the Northern zone.

4.1.2. Central zone (Brussels, Milan, Madrid)

In the Central zone, Irrdir on the vertical surface is relatively constant regardless of the season. The values of Irrdir in spring, summer, fall and winter obtained from yearly solar analyses are close although they differ in terms of angular distribution (Fig. 6 and Table 7).

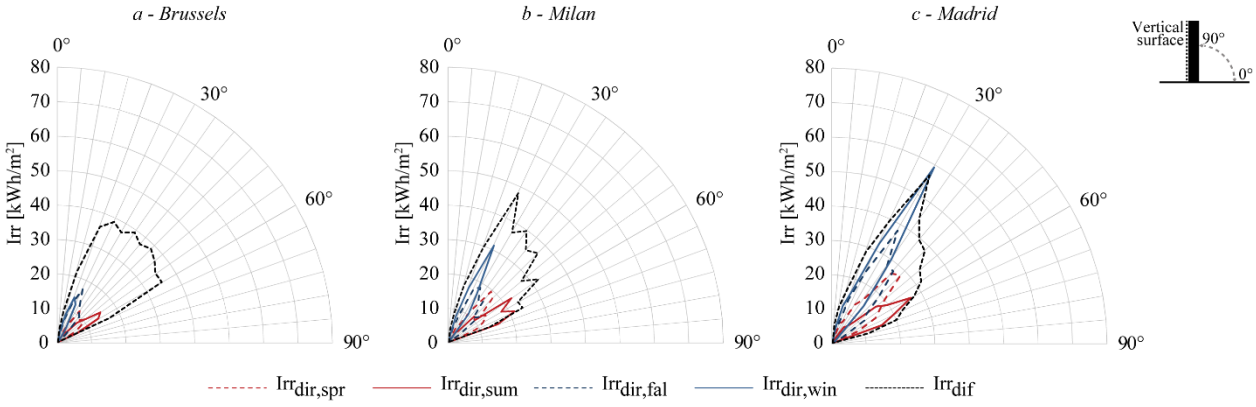

Figure 6 Yearly data of angular distribution of the Irr_{dif} and Irr_{dir} on a vertical surface in the Central zone. The Irr_{dir} data is presented in seasonal contributions.

Published in *Solar Energy 176, pp. 194-210, 2018*
DOI: *10.1016/j.solener.2018.10.003*

Table 7 Summary of the yearly outcomes of number of hours of daylights, the Irr_{dir} and the Irr_{gl}. For each season are reported the highest value of the Irr_{dir} collected by the vertical surface considering an angular range of 10°, 40°, 90° respectively, the Irr_{gl} and the Irr_{dir}/Irr_{gl} ratio.

Case study cities	Number of hours of daylighting [h]	$Irr_{dir,yr}$ [kWh/m²]	$Irr_{gl,yr}$ [kWh/m²]	Season	Irr_{dir} 10° [kWh/m²]	Irr_{dir} 40° [kWh/m²]	Irr_{dir} 90° [kWh/m²]	Irr_{gl} [kWh/m²]	Irr_{dir}/Irr_{gl} [%]
Brussels	4,404	248	628	Spring	20	62	65	182	36
				Summer	28	61	62	203	31
				Fall	30	73	75	158	47
				Winter	26	44	44	85	52
Milan	4,405	447	864	Spring	41	110	119	247	48
				Summer	44	116	118	244	49
				Fall	39	116	116	211	55
				Winter	53	93	93	161	58
Madrid	4,393	636	1,058	Spring	54	141	160	282	57
				Summer	46	117	121	234	52
				Fall	65	172	186	295	63
				Winter	91	167	169	246	69

In Brussels, the Irrdir raises from summer to fall mainly because of the variation in the sun path geometry. The sun remains closer to the horizon during fall, achieving a maximum azimuth angle equal to 65° in summer and 50° in fall, while the peak is registered in fall at 25° (17 kWh/m2) (Fig. 8a). In terms of Irrdir/Irrgl, Brussels represents the worst case, hardly reaching percentages higher than 50%, and with a maximum of 52% in winter (Table 7). The main cause is the high cloudiness index that is the highest in the Central zone (Fig. 7). Furthermore, this aspect also affects the yearly distribution of Irrdif, which in Brussels is mostly constant during the whole year (Fig. 6a).

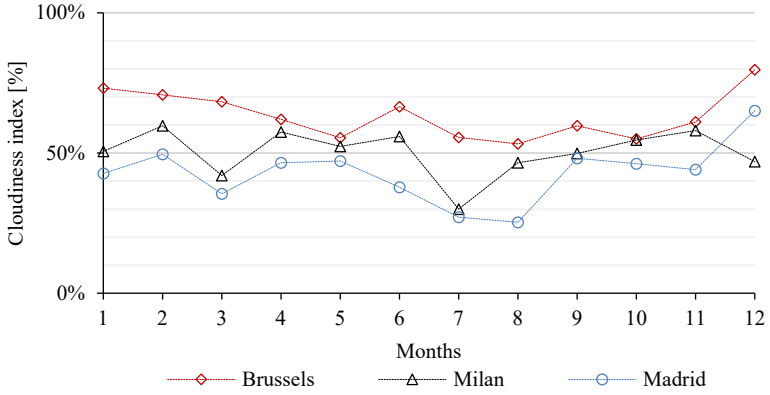

Figure 7 Monthly cloud coverage values calculated for each location of the Central zone.

The analyses conducted in Milan showed that the Irrdir is practically constant along the year (from 116 kWh/m2 in fall to 118 kWh/m2 in spring and 119 kWh/m2 in summer), with the exception of winter (93 kWh/m2) (Table 7).

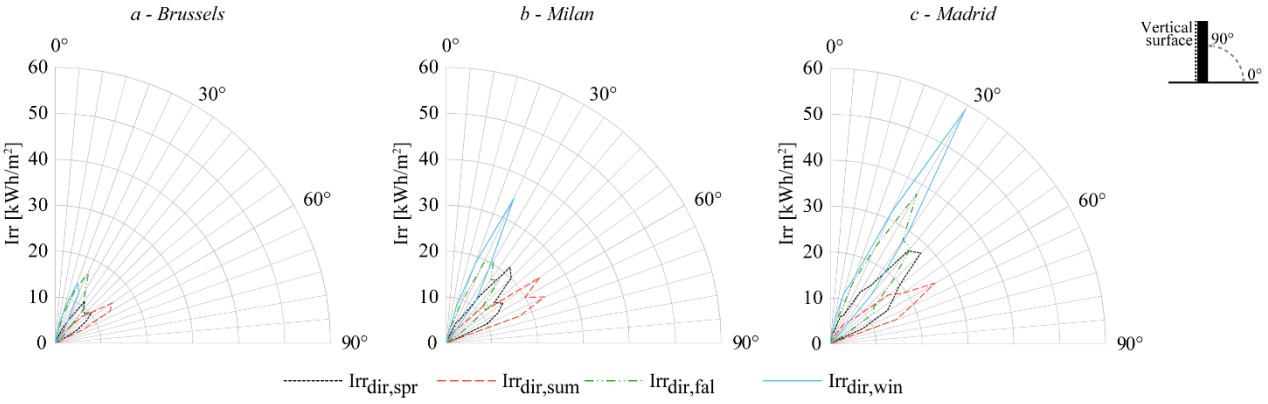

Published in *Solar Energy 176, pp. 194-210, 2018*
DOI: *10.1016/j.solener.2018.10.003*

Figure 8 Angular yearly distribution of Irr_{dir} on the vertical surface in the Central zone.

In Madrid, the Irrdir in summer reaches 121 kWh/m2, which is the lowest value of the year (Table 7). This is mainly due to the sun azimuth angle that is higher in summer so that the sunrays hit the vertical surface with a mostly parallel direction (Fig. 8c). This is also confirmed by the peak of Irrdir, which in Madrid is registered in winter at 30° (59 kWh/m2), when the sun angle is lower and the sunrays more perpendicular to the vertical surface.

4.1.3. Southern zone (Valletta, Cairo, Doha)

The yearly solar analyses underline that the solar geometry in the Southern zone shows a predominance of sunrays parallel to the façade in spring and in summer.

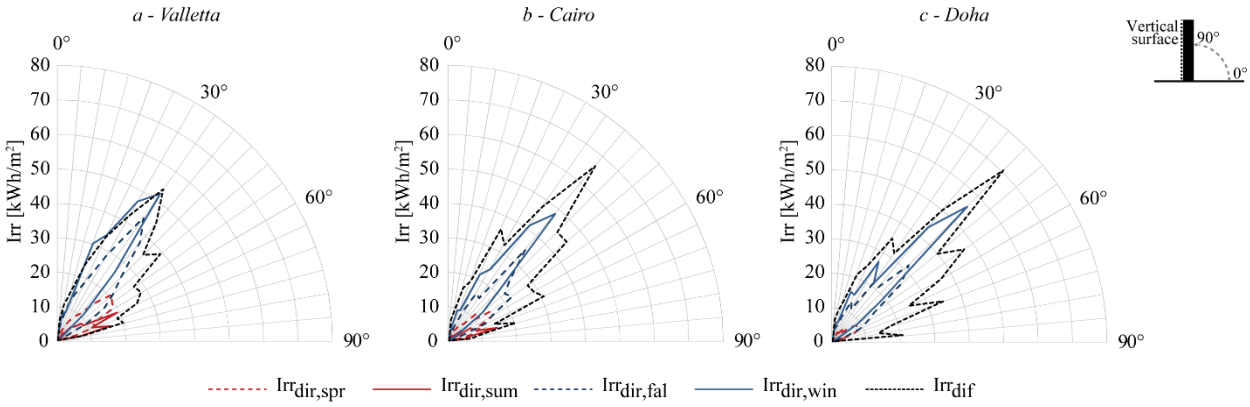

Figure 9 Yearly data of angular distribution of the Irr_{dif} and Irr_{dir} on a vertical surface in the Southern zone. The Irr_{dir} data is presented in seasonal contributions.

This is the main cause for the low amount of available Irrdir on the vertical surface in spring and in summer; while in fall and in winter, the vertical surface is found to be able to collect a higher amount of Irrdir (Fig. 9 and Table 8).

The yearly analysis for Valletta confirms that the predominant contribution of Irrdir is during the cold seasons: more than two third of the annual Irrdir (680 kWh/m2) is collected from September to February. Furthermore, all the seasonal values of Irrdir collected on the vertical surface are always higher or equal to the values in Doha or in Cairo (Table 7).

Table 8 Summary of the yearly outcomes of number of hours of daylights, the Irr_{dir} and the Irr_{gl}. For each season are reported the highest value of the Irr_{dir} collected by the vertical surface considering an angular range of 10°, 40°, 90° respectively, the Irr_{gl} and the Irr_{dir}/Irr_{gl} ratio.

Case study cities	Number of hours of daylighting [h]	$Irr_{dir,yr}$ [kWh/m^2]	$Irr_{gl,yr}$ [kWh/m^2]	Season	Irr_{dir} 10° [kWh/m^2]	Irr_{dir} 40° [kWh/m^2]	Irr_{dir} 90° [kWh/m^2]	Irr_{gl} [kWh/m^2]	Irr_{dir}/Irr_{gl} [%]
Valletta	4,392	680	1,107	Spring	40	115	138	253	55
				Summer	29	76	87	193	45
				Fall	81	205	234	342	68
				Winter	98	215	220	318	69
Cairo	4,380	537	992	Spring	30	81	102	225	45
				Summer	23	53	58	152	38
				Fall	59	160	182	303	60
				Winter	89	185	194	311	62
Doha	4,386	481	978	Spring	17	49	62	190	33
				Summer	5	15	17	133	13
				Fall	58	149	181	310	59
				Winter	99	205	220	345	64

Published in *Solar Energy 176, pp. 194-210, 2018*
DOI: *10.1016/j.solener.2018.10.003*

There are two reasons that explain these results: on one hand, the sunrays have a parallel direction to the analyzed vertical surface for most part of the year in Cairo and in Doha; on other hand, the values of cloud coverage in Valletta are intermediate between the ones in Cairo and in Doha almost for all the period including spring and summer (Fig. 10).

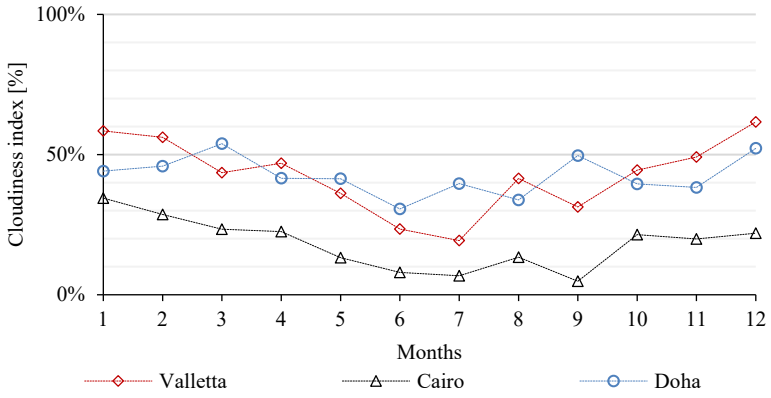

Figure 10 Monthly cloud coverage values calculated for each location of the Southern zone.

As far as the Irrdir/Irrgl value is concerned, this ratio is on average higher in Valletta than in the Northern and Central zones: the values are constantly above the 50% – from 55% in spring to 69% in winter – except in summer, when it is down to 45% (Table 8). Furthermore, in fall and in winter, the Irrdir/Irrgl in Valletta result to be the highest registered in the Southern zone, although this value in Cairo and in Doha is always around or higher than 60% (Table 8). Contrary, in Doha the lowest value equal to 13% of all the zones is registered (Table 8), while the highest values of seasonal amount of Irrdir equal to 220 kWh/m2 is reached in the winter, with the highest contribution provided from September to February. The peak value is registered at 45° (32 kWh/m2) in the fall (Fig. 11c).

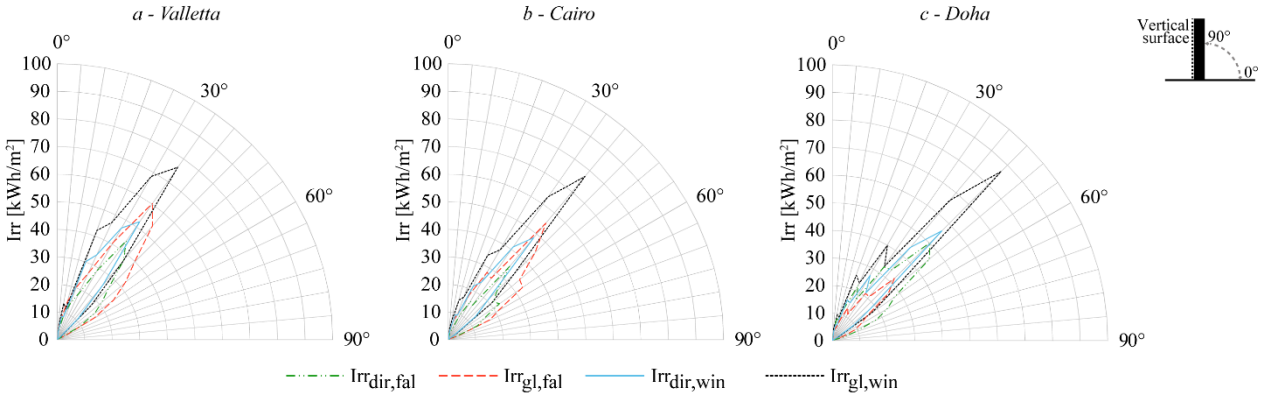

Figure 11 Angular yearly distribution of Irr_{dir} on the vertical surface in the Southern zone.

4.2. Potentials for application of RR materials on vertical surfaces

The Irrdir/Irrgl ratio allows the effectiveness of RR material to be evaluated: a higher value of Irrdir/Irrgl indicates a higher potential for reflecting back the incoming radiation, and consequently impacts on the mitigation of the UHI effect. As far as this aspect is concerned, the activation of the retro-reflection property of RR materials depends therefore mostly

Published in *Solar Energy 176, pp. 194-210, 2018*
DOI: *10.1016/j.solener.2018.10.003*

on the solar geometry. Furthermore, the periods of the year when the RR materials applied on the vertical surface could guarantee the highest level of performance are different in each zone.

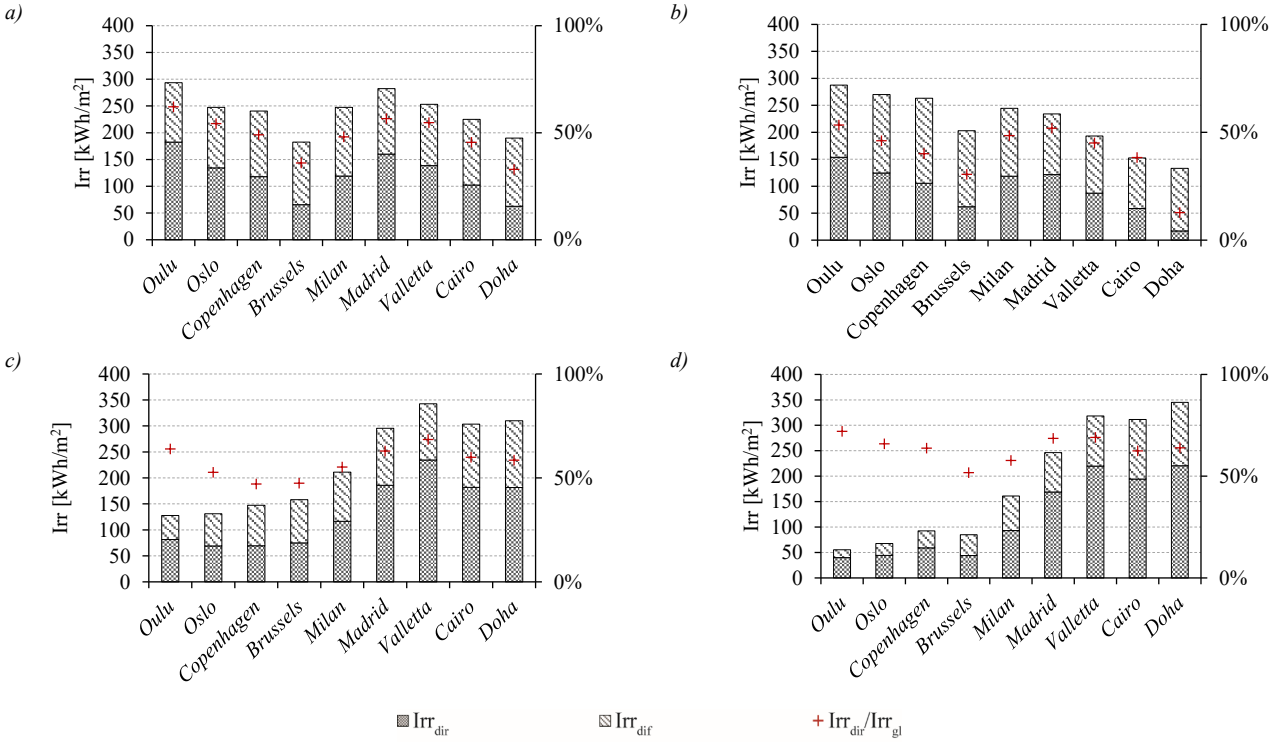

Figure 12 Assessment of solar irradiation collected by the vertical surface during spring (a), summer (b), fall (c), and winter (d).

When considering the spring season, the Irrdir/Irrgl is higher than 50% (Fig. 12a) in only four locations (Oulu and Oslo in the Northern zone, in Madrid for Central zone and in Valletta for Southern zone). This means that more than 50% of the impinging Irrgl on a vertical surface can be retro-reflected. In summer, because of the solar geometry, the values of Irrdir/Irrgl are in the range between 10% in Doha and 55% in Madrid and Oulu, whereas for the other locations the Irrdir/Irrgl remains lower than 50%. Therefore, the impact of Irrdir on the vertical surface is lower in the summer than in other periods of the year, as also demonstrated by the lowest values of Irrdir/Irrgl (Fig. 12b).

However, it is worth noting that the RR materials perform best in spring and in summer in the Northern zone, when up to 70% of the yearly Irrdir is collected by the vertical surface (Fig. 13a). This is due to the sun position, sun path and sun angles that in these periods of the year allows longer exposure of the façade to the sun. Conversely, in the Southern zone, almost the same percentage (70%) of Irrdir is collected in fall and in winter (Fig. 13a).

Published in *Solar Energy 176, pp. 194-210, 2018*
DOI: *10.1016/j.solener.2018.10.003*

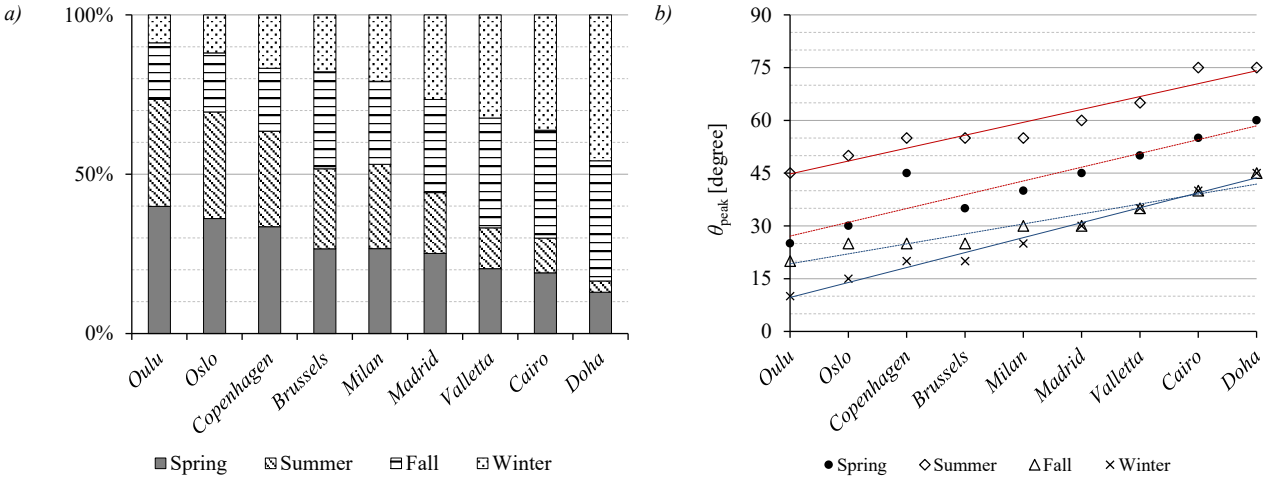

Figure 13, Seasonal Irr_{dir} contributions to the yearly balance (a) and angle of incidence on the vertical surface of the seasonal peaks (a).

Moving toward the Equator, the increasing azimuth angle in the summer affects significantly the intensity of Irrdir, which is characterized by the lowest yearly values. On the contrary, at these latitudes, it should be necessary to mitigate the urban overwarming during the cold seasons given the highest values of Irrdir in fall and in winter (Fig. 13a), and the relatively high outdoor air temperatures in these seasons. When it comes to the Central zone, the yearly Irrdir is equally distributed among the four seasons (around 25% each) for all the locations (Fig. 13a); therefore, a RR material can be effective through the whole year given that there is not prevalent season. Brussels represents an exception since in this climate context the component of Irrdir is always lower than the Irrdif. In this case, the RR technology demonstrates to be a less effective strategy for the mitigation of the UHI phenomenon (Fig. 12a–d).

The assessment of the peaks and of the angular distribution of solar irradiation incident on the vertical surface, shows a linear relation from the Northern zone to the Southern zone, in all the seasons (Fig. 13b). Furthermore, the results of this investigation confirm that the retro-reflection should be activated:

- in the summer and the spring in the range 25–55°, in the Northern zone;
- in the summer and in the spring in the range 30–70°, in the Central zone;
- in the fall and in winter between 25° and 55° in the Southern zone.

a – angular range of 10° wide *b – angular range of 40° wide* *c – angular range of 90° wide*

Published in *Solar Energy 176, pp. 194-210, 2018*
DOI: *10.1016/j.solener.2018.10.003*

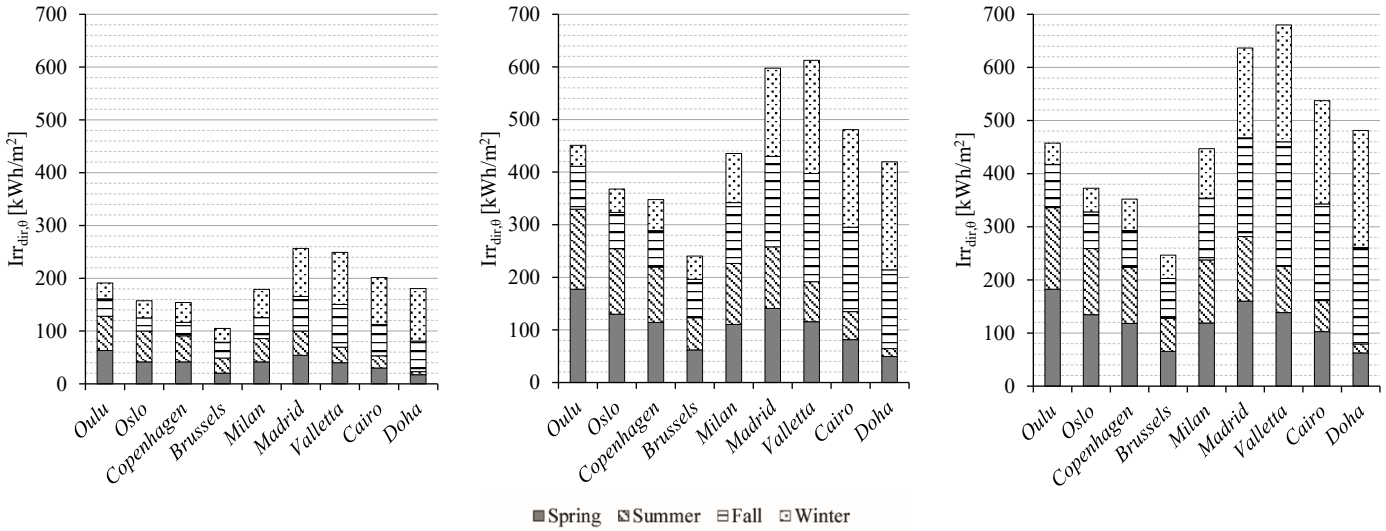

Figure 14 Annual Irr_{dir} on a vertical surface calculated on angular ranges of 10° (a), 40° (b), 90° (c), around the seasonal peaks.

The annual Irrdir calculated on angular ranges of 10° (Fig. 14a), 40° (Fig. 14b), 90° (Fig. 14c) around the seasonal peaks, highlights that a significant fraction of the yearly Irrdir is included within an angular range of 40°. Therefore, an RR material characterized by a perfect retro-reflection behaviour with a constant range of 40° (but with different absolute values according to the different locations) can be able to retro-reflect almost the totality of the incident Irrdir through the year. The Irrdir distributed in the remaining 50° is more significant for the application of RR material in latitudes lower than Milan, such as Madrid, and in all locations of the Southern zone, where a larger range of angular distribution of Irrdir could be effectively exploited (Fig. 14).

4.3. Solar irradiation analyses on horizontal surface

4.3.1. Northern zone (Oulu, Oslo, Copenhagen)

The data regarding Irrdir on the horizontal surface obtained from the annual angular distribution (Fig. 15 and Table 9) highlights that the major contribution is seen in the Northern zone in the spring and in the summer.

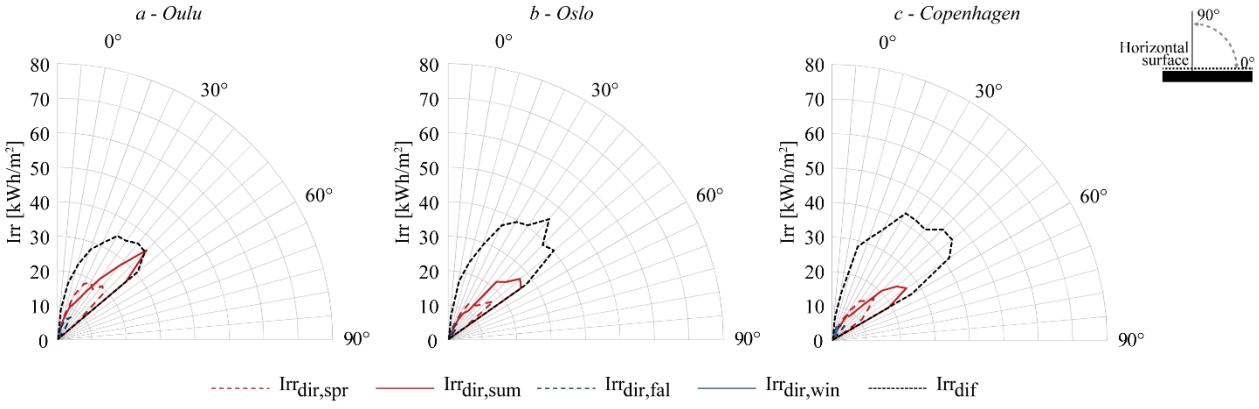

Figure 15 Yearly data of angular distribution of the Irr_{dif} and Irr_{dir} on a horizontal surface in the Northern zone. The Irr_{dir} data is presented in seasonal contributions.

Table 9 Summary of the yearly outcomes of number of hours of daylights, the Irr_{dir} and the Irr_{gl}. For each season are reported the highest value of the Irr_{dir} collected by the horizontal surface considering an angular range of 10°, 40°, 90° respectively, the Irr_{gl} and the Irr_{dir}/Irr_{gl} ratio.

Published in *Solar Energy 176, pp. 194-210, 2018*
DOI: *10.1016/j.solener.2018.10.003*

Case study cities	Number of hours of daylighting [h]	$Irr_{dir,yr}$ [kWh/m^2]	$Irr_{gl,yr}$ [kWh/m^2]	Season	Irr_{dir} 10° [kWh/m^2]	Irr_{dir} 40° [kWh/m^2]	Irr_{dir} 90° [kWh/m^2]	Irr_{gl} [kWh/m^2]	Irr_{dir}/Irr_{gl} [%]
Oulu	4,428	477	892	Spring	58	180	186	325	57
				Summer	96	230	236	446	53
				Fall	20	45	45	98	46
				Winter	7	9	10	23	41
Oslo	4,419	363	878	Spring	47	129	133	300	44
				Summer	79	186	189	432	44
				Fall	14	32	32	112	28
				Winter	6	9	9	34	26
Copenhagen	4,411	379	981	Spring	47	128	136	325	42
				Summer	75	182	188	461	41
				Fall	14	39	39	139	28
				Winter	10	39	39	55	29

During these seasons, in Oulu, the Irrdir angular distribution shows the seasonal peaks respectively at 40° in spring (30 kWh/m2) and 45° in summer (55 kWh/m2) (Fig. 16a), while the total amount of Irrdir collected by the horizontal surface equals 186 kWh/m2 in spring and 236 kWh/m2 in summer (Table 9). These values are the highest in the Norther zone and they correspond to 57% of Irrgl in spring – the highest Irrdir/Irrgl ratio – and 53% in summer (Table 9).

In Oslo, in spring and in summer, the effect of the high cloud coverage is confirmed by the Irrdir/Irrgl ratio values calculated on the horizontal surface, which ranges between 26% (winter) (the lowest value in the Northern zone) and 44% (in spring and summer). Copenhagen has the lowest value (42%) of Irrdir/Irrgl ratio in the warm seasons in Northern zone (Table 9).

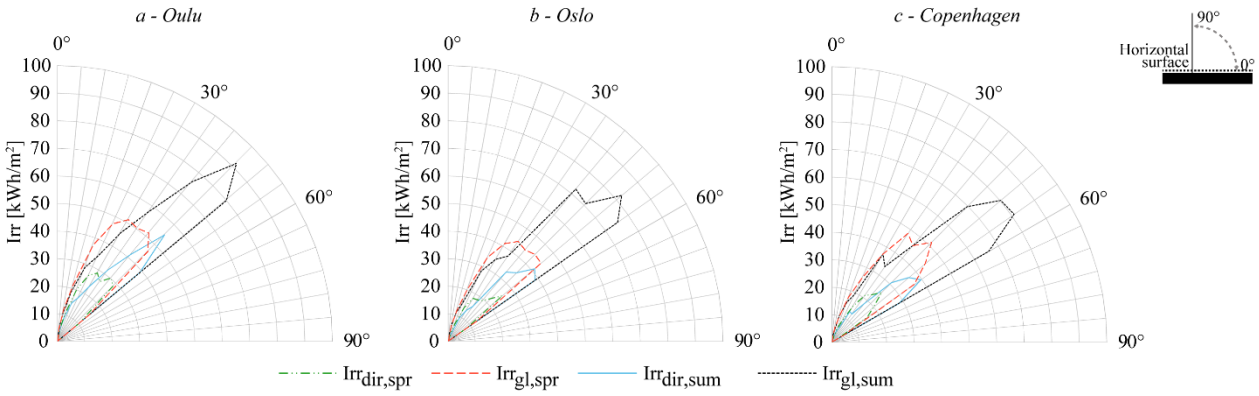

Figure 16 Angular distribution of both Irr_{dir} and Irr_{gl} on the horizontal surface in spring and in summer in the Northern zone.

4.3.2. Central zone (Brussels, Milan, Madrid)

In the Central zone, the values of Irrdir incident on a horizontal surface in summer are the most relevant (Fig. 17 and Table 10).

Published in *Solar Energy 176, pp. 194-210, 2018*
DOI: *10.1016/j.solener.2018.10.003*

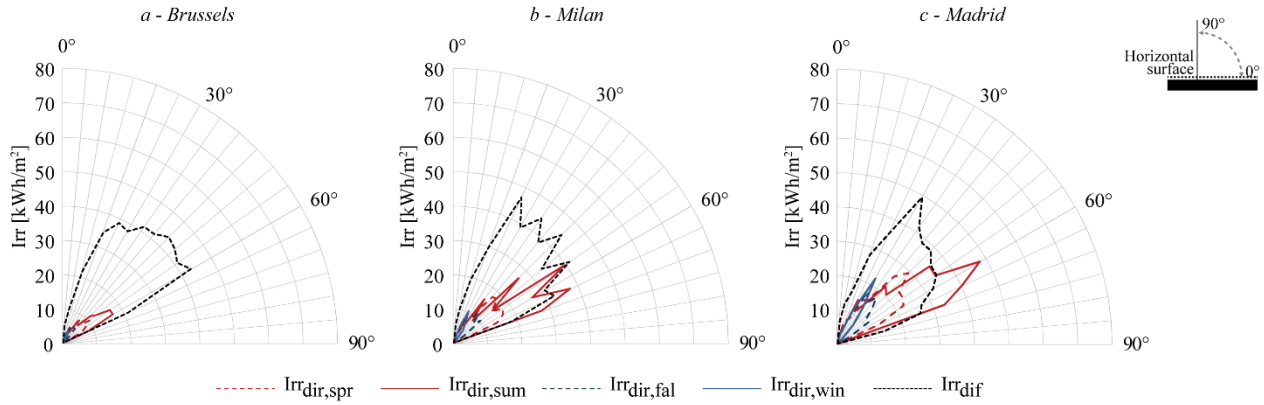

Figure 17 Yearly data of angular distribution of the Irr_{dir} on a horizontal surface and Irr_{dif} in the Central zone. The Irr_{dir} data is presented in seasonal contributions.

In Brussels, the Irrdir calculated on a horizontal surface registered the lowest values of Irrdir/Irrgl ratios in relation to all locations: the average of the seasonal Irrdir/Irrgl ratios is around 30%, and never higher than 35% (Table 10). Regarding the seasonal amounts of Irrdir, the seasonal peaks are singular and they are shown at 50° in spring, 55° in summer, 25° in fall, and 20° in winter (Figs. 17a and 18a). Whereas, in Milan the angular distribution of Irrdir shows the presence of several local peaks in all seasons, with the maximum at 55° in summer (Figs. 17b and 18b).

Table 10 Summary of the yearly outcomes of number of hours of daylights, the Irr_{dir} and the Irr_{gl}. For each season are reported the highest value of the Irr_{dir} collected by the horizontal surface considering an angular range of 10°, 40°, 90° respectively, the Irr_{gl} and the Irr_{dir}/Irr_{gl} ratio.

Case study cities	Number of hours of daylighting [h]	$Irr_{dir,\ yr}$ [kWh/m²]	$Irr_{gl,yr}$ [kWh/m²]	Season	Irr_{dir} 10° [kWh/m²]	Irr_{dir} 40° [kWh/m²]	Irr_{dir} 90° [kWh/m²]	Irr_{gl} [kWh/m²]	Irr_{dir}/Irr_{gl} [%]
Brussels	4,404	287	917	Spring	27	81	89	290	31
				Summer	50	124	135	401	33
				Fall	17	46	46	157	29
				Winter	10	16	16	69	24
Milan	4,405	644	1,291	Spring	53	172	187	397	47
				Summer	99	293	318	553	57
				Fall	30	92	95	221	43
				Winter	25	43	43	120	35
Madrid	4,393	967	1,617	Spring	82	250	284	489	58
				Summer	132	370	427	642	66
				Fall	48	150	161	303	40
				Winter	52	93	93	183	51

In Madrid, the Irrdir in summer reaches 427 kWh/m2, which is by far the highest value among the seasonal ones in the whole Central zone (Table 10).

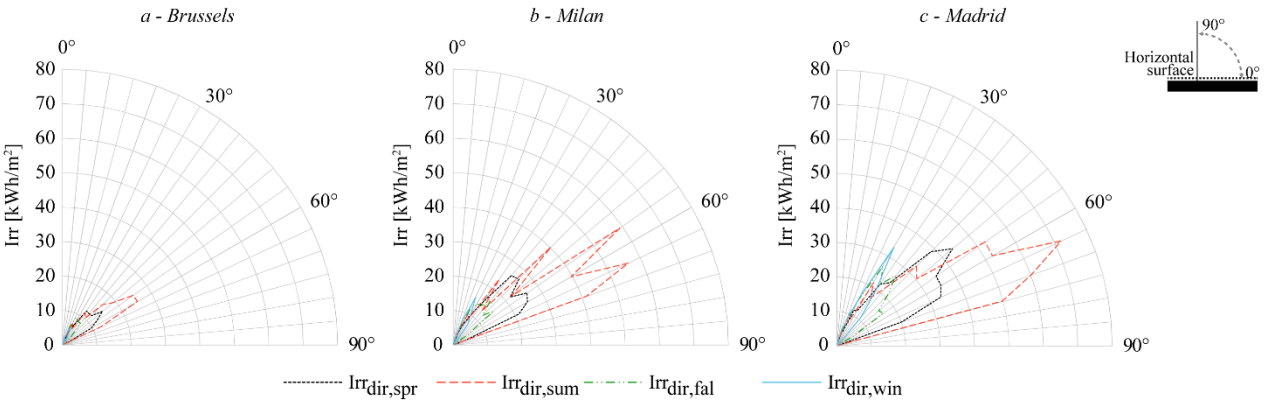

Figure 18 Angular distribution of direct solar Irr_{dir} on the horizontal surface through the year in the Central zone.

Published in *Solar Energy 176, pp. 194-210, 2018*
DOI: *10.1016/j.solener.2018.10.003*

Madrid also presents the highest Irrdir/Irrgl values, which are equal to 66% in summer and 58% in spring (Table 10). Furthermore, it is worth noting that only one third of the yearly Irrdir (967 kWh/m2) is collected during fall and winter.

4.3.3. Southern zone (Valletta, Cairo, Doha)

The yearly solar analyses underline that the solar geometry in the Southern zone shows a predominance of the Irrdir to the horizontal surface during the spring and the summer (Fig. 19 and Table 11).

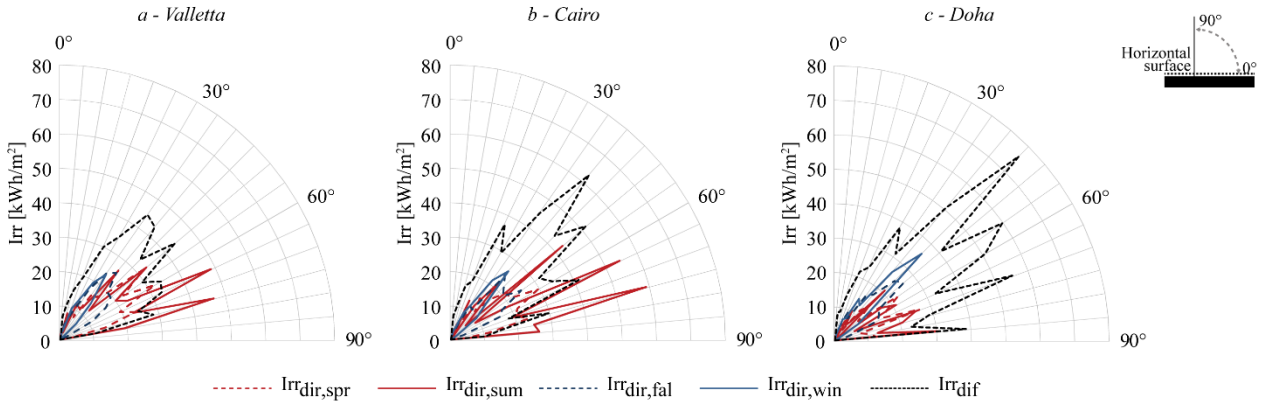

Figure 19 Yearly data of angular distribution of the Irr_{dif} and Irr_{dir} on a horizontal surface in the Southern zone. The Irr_{dir} data is presented in seasonal contributions.

Table 11 Summary of the yearly outcomes of number of hours of daylights, the Irr_{dir} and the Irr_{gl}. For each season are reported the highest value of the Irr_{dir} collected by the horizontal surface considering an angular range of 10°, 40°, 90° respectively, the Irr_{gl} and the Irr_{dir}/Irr_{gl} ratio.

Case study cities	Number of hours of daylighting [h]	$Irr_{dir,\ yr}$ [kWh/m²]	$Irr_{gl,yr}$ [kWh/m²]	Season	Irr_{dir} 10° [kWh/m²]	Irr_{dir} 40° [kWh/m²]	Irr_{dir} 90° [kWh/m²]	Irr_{gl} [kWh/m²]	Irr_{dir}/Irr_{gl} [%]
Valletta	4,392	1,155	1,811	Spring	81	270	340	536	63
				Summer	106	345	443	657	67
				Fall	73	211	235	373	63
				Winter	63	134	136	244	56
Cairo	4,380	1,175	1,919	Spring	75	245	319	552	58
				Summer	125	378	465	667	69
				Fall	69	218	240	408	59
				Winter	69	144	150	291	51
Doha	4,386	971	1,867	Spring	63	185	255	517	49
				Summer	68	198	275	563	49
				Fall	76	204	246	438	56
				Winter	92	185	195	347	56

The yearly analysis of Valletta confirmed that the predominant contribution to Irrdir takes place in the spring (340 kWh/m2) and in the summer (443 kWh/m2) (Table 11). The angular distribution of Irrdir in the summer (Fig. 20 a) shows three local peaks within a range of 25° (from 50° to 75°). Furthermore, the Irrdir/Irrgl ratios are always higher than 60%, with the exception of the winter (Table 11).

In Cairo, the seasonal amount of Irrdir collected by the horizontal surface and its angular distribution with several peaks between 50° and 75°does not particularly differ from Valletta (Table 11 and Fig. 20b).

Doha represents the exception in this zone because of the lack of a predominance of Irrdir collected in the spring and in the summer, showing seasonal values of Irrdir very close to one another (Table 11). The lower Irrdir available in Doha

Published in *Solar Energy 176, pp. 194-210, 2018*
DOI: *10.1016/j.solener.2018.10.003*

is partially due to the higher cloudiness index (Fig. 10), as demonstrated by the Irrdir/Irrgl ratios (around 50% through the year). Nevertheless, the yearly Irrgl value (1867 kWh/m2) is aligned with the corresponded quantities calculated in Valletta (1811 kWh/m2) and in Cairo (1919 kWh/m2).

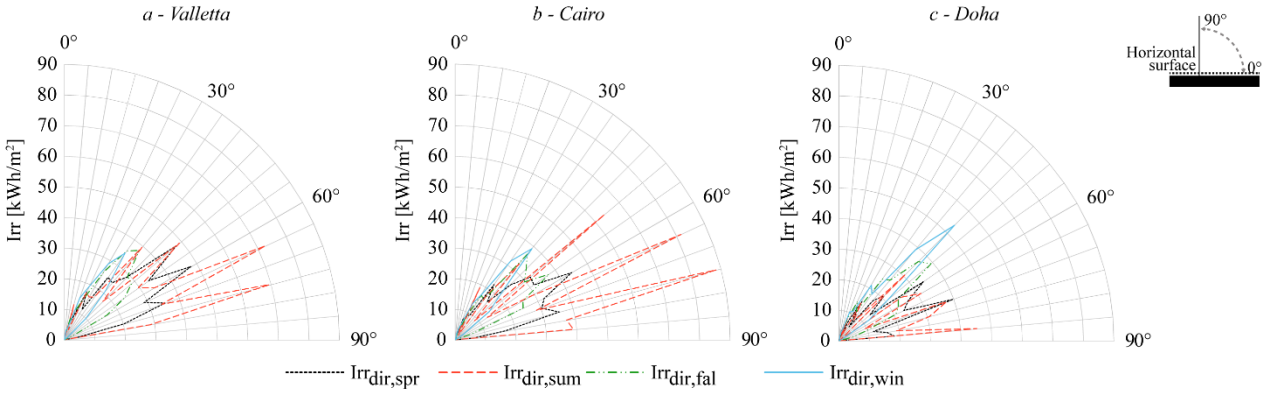

Figure 20 Angular distribution of Irr_{dir} incident on the horizontal surface through the year in the Southern zone.

4.4. Potentials for application of RR materials on horizontal surfaces

The results obtained through the solar irradiation analyses on the horizontal surface confirmed that Irrdir values observed during cold seasons are lower than the ones estimated for the vertical surface due to the solar geometry.

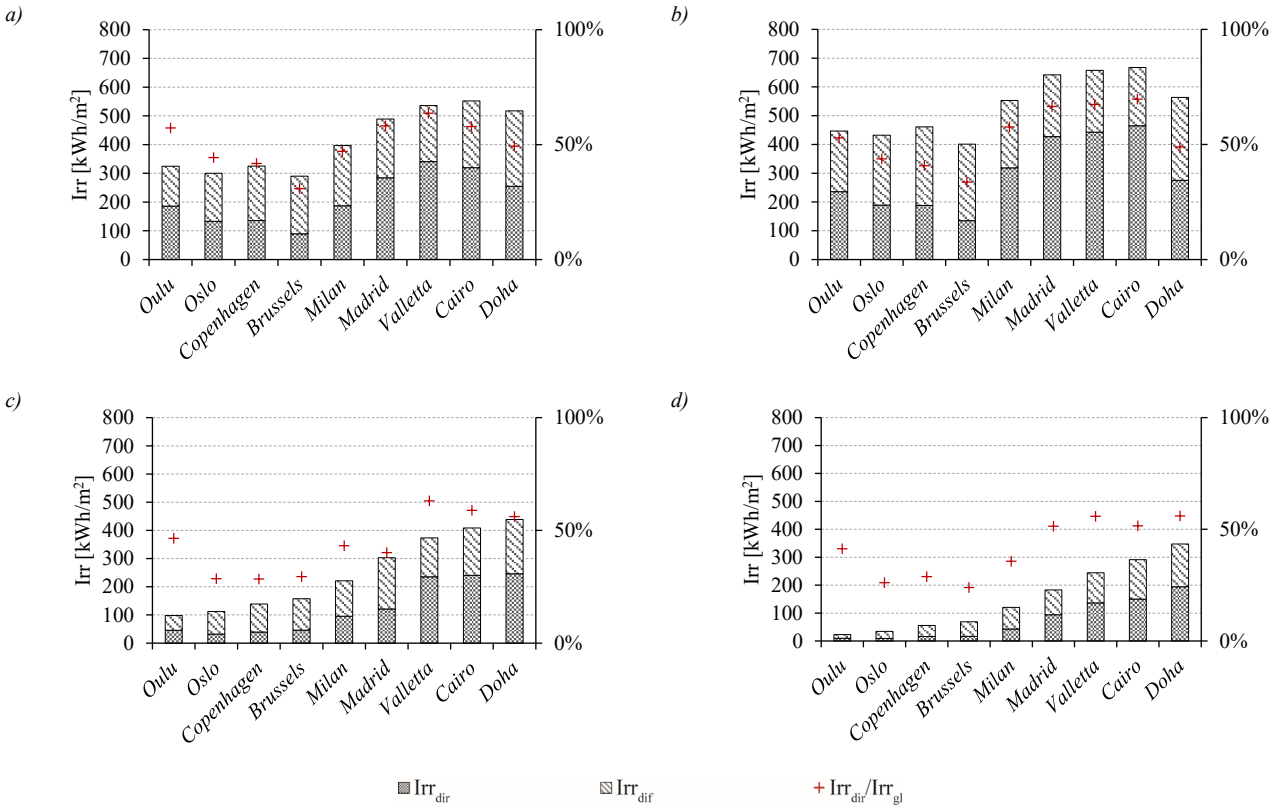

Figure 21 Assessment of solar irradiation collected by the horizontal surface during spring (a), summer (b), fall (c), and winter (d).

In spring, the Irrdir/Irrgl is lower than 50% (Fig. 21a) in only four locations (Oslo and Copenhagen in the Northern zone, Brussels and Milan in the Central zone). A similar result can be observed during summer (Fig. 21b), with the

Published in *Solar Energy 176, pp. 194-210, 2018*
DOI: *10.1016/j.solener.2018.10.003*

exception of Milan, whose Irrdir/Irrgl ratio reaches 57%. Furthermore, in summer the impact of RR materials applied on horizontal surfaces seems to be significant in Madrid, Valletta and Cairo, where the maximum Irrdir/Irrgl values are achieved (from 66% to 69%). During the rest of the year, the Irrdir/Irrgl ratios remain lower than 50% in all the locations, with the exception of the Southern zone (in fall and in winter) and of Madrid (only in winter) (Fig. 21c and d).

The exploitation of RR materials on the horizontal surface is revealed to be advantageous in spring and in summer at all latitudes, since the Irrdir values in those seasons range from 50% in Doha to 90% in Oulu (Fig. 22a). It is observed that in Doha the yearly Irrdir is equally distributed among the four seasons (around 25% each), similarly to what is seen in the Central zone for a vertical surface (Fig. 13a).

The peaks of the angular distribution of Irrdir in summer and in winter can be considered, with a relatively good approximation, linearly correlated with the latitude. However, such a behaviour is not recorded in spring and in fall (Fig. 22b), when the peaks along the different locations are more irregularly distributed. As a matter of fact, it is worth mentioning that for both vertical and horizontal surfaces, the linear trend lines of the peaks of the angular distribution of Irrdir, in summer and in winter, are almost parallel with a gap of 30° (Fig. 22b).

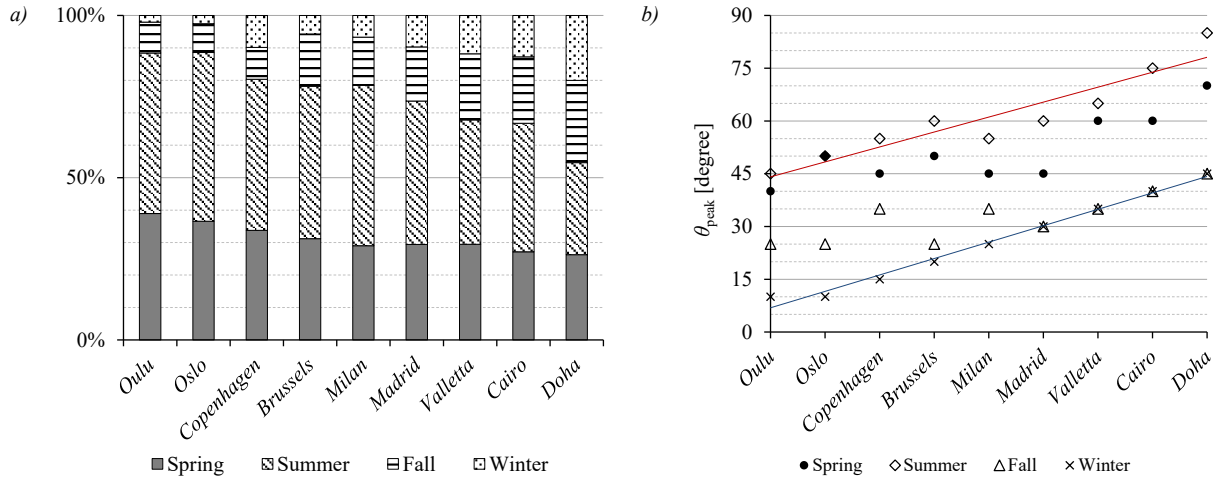

Figure 22 Angle of incidence in the horizontal surface of the seasonal peaks calculated considering an angular range 10° wide (a), and seasonal direct solar irradiation contributions to the yearly balance (b).

The assessment of seasonal peaks of Irrdir and their angular distribution on a horizontal surface, confirmed that retro-reflection should be activated:

- in spring and in summer at all latitudes;
- in fall and in winter in the Southern zone.

The angular range of activation is between 35° and 55° in the Northern zone, between 30° and 70° in the Central zone, and between 0° and 90° in the Southern zone (no selective behavior needed). In Fig. 23 c the seasonal values of Irrdir considering an angular range varying from 10° (Fig. 23a) to 40° (Fig. 23b) and 90° around the seasonal peaks are shown. It is worth observing that almost the entire direct radiation is collected in an angular range of 40° (Fig. 23b) in all the locations in the Northern zone, while in the Central zone this happens only in Brussels. On the contrary, Irrdir is

Published in *Solar Energy 176, pp. 194-210, 2018*
DOI: *10.1016/j.solener.2018.10.003*

characterized by a wider angular distribution in Milan and Madrid, in the Central zone, and in the entire Southern zone. As a result, RR materials to be applied to horizontal surfaces in the Southern zone should present an angular range wider than 40° in order to exploit the maximum mitigation potential throughout the year. This implies that the existing RR materials are not very efficiently exploitable in the southernmost locations since they present a perfect RR behavior within an angular range 60° wide (Castellani et al., 2017).

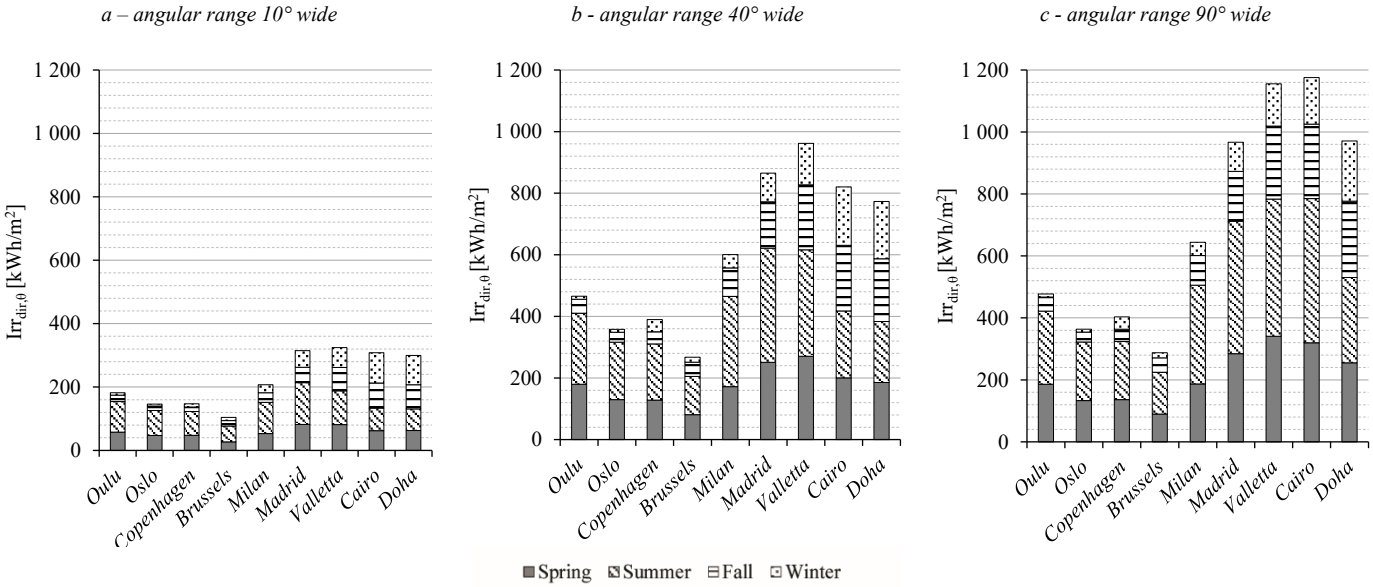

Figure 23 Seasonal peaks in horizontal surface ($Irr_{dir,\theta}$) calculated on angular ranges equal to 10° (a), 40° (b), 90° (c).

4.5. Limitations of the study

The main limitation of this study is related to the system boundary adopted in the investigation, which is to say a building inserted in an unobstructed environment without any urban surrounding (i.e. urban canyon and building blocks). The boundary condition where the building is surrounded by other buildings was not investigated, since the aim of this work was to identify optimal selective properties of RR materials, as well as maximum potential for application, and these are both independent from any specific urban canyon configuration or urban surrounding. This means that the values for Irrdir presented in this paper are the maximum values of solar radiation that can be retro-reflected. Such a value can be lowered in an urban canyon configuration or complex urban surrounding because of the direct shadow created by other buildings. However, the advantages provided by the application of RR materials compared to the traditional cool materials are particularly notable when applied to urban canyon configurations (Rossi et al., 2015). Therefore, the application of RR materials on the surfaces of urban canyons will be investigated in the next step of the research activity in order to take into account all mutual solar inter-building effects.

The second limitation is related to the selection of a unique exposure of the vertical surface: in this work, only the south façade was presented. As highlighted in Table 2, this choice is again based on the aim of considering the maximum

potential of the RR technology. Nonetheless, when integrated in urban canyon configurations or complex urban environments, the RR materials might find suitable applications also on façades with different exposures (e.g. south-west, west, south-east, east). Optimal properties for RR materials applied to these orientations will be investigated, and their impact assessed, in the second phase of the research activity, when the simulations will be scaled-up to study districts.

A third limitation is related to the methodology. All the tools used in the investigation are validated simulation environments. In particular, when it comes to geometrical aspects of solar radiations, which is a crucial aspect of this research, it is reasonable to expect that the degree of accuracy of the adopted tools is very high, as these are based on models established (and verified) a very long time ago. However, when it comes to the balance between the Irrdir and Irrgl on a surface, this value is affected by the weather data file used in the simulation. In this activity, the TMY for each location was considered, as the use of TMY data is the most common procedure, and the most accepted one too, for the estimation of performance of building or building components under realistic dynamic boundary conditions. However, the use of one weather data file instead of another, for the same location, might lead to different balances between direct and indirect solar radiation – hence on the share of the total solar radiation that an RR can act on. The outcomes of this study have shown that the cloud coverage level may have a relatively large impact – see the case of Brussels (Section 4.3.2). However, this uncertainty factor does not affect the optimal angular properties of RR materials (i.e. the primary knowledge gains of the research activity presented in this paper): these properties are the same regardless of the balance between direct and indirect solar irradiation on the surface where the RR material is applied. When moving to the district level scale through the simulation of urban canyon configurations, a sensitivity analysis where the cloud coverage index is varied (and consequently the balance between direct and indirect solar radiation) can be a suitable strategy to provide a more comprehensive insight on the actual performance of RR materials under real urban configurations.

5. Best practices for the use RR materials in different climate zones/latitudes

As shown in (Fig. 24), the difference between the Irrdir reaching the vertical and the horizontal surface increases from the Northern zone to the Southern zone.

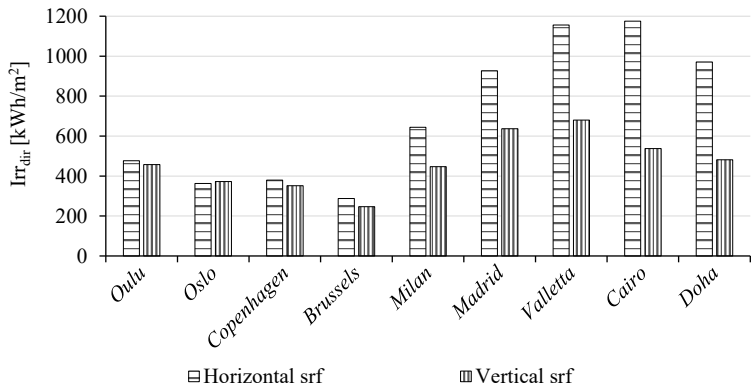

Figure 24 Comparison of the annual direct solar irradiation between horizontal and vertical case study.

Published in *Solar Energy 176, pp. 194-210, 2018*
DOI: *10.1016/j.solener.2018.10.003*

The cities of Oulu, Oslo, Copenhagen, and Brussels are characterized by a difference between Irrdir collected by the vertical surface and Irrdir collected by the horizontal surface – calculated on a yearly basis – lower than 40 kWh/m2. The minimum difference is registered in Oslo, where the vertical surface turns out to be able to collect more Irrdir than the horizontal surface (Fig. 24). On the other hand, in the other case study cities, it is shown that the application of RR materials on a horizontal surface would be more efficient, given that almost the double of the Irrdir could be reflected back compared to the installation of RR materials on the vertical surface.

The successful application of RR materials on the vertical surface in the Northern zone requires that an ideal RR material exhibits the RR behavior in an angular interval in the range 25–55°. This is the optimal range to reflect back the solar irradiation in the spring and in the summer (Table 12).

In the Central zone, a RR-enhanced vertical surface would not be very effective in Brussels because only a small fraction of the total solar irradiation can be tackled through a RR system. On the contrary, the application of these materials is shown to be more effective in Milan and Madrid. In these two cities, a vertical surface with an RR behaviour in the angular interval from 30° and 70° allows absorbing the direct irradiation in the winter, and reflectinga large amozarmest periods.

In the Southern zone, where the range of the angular distribution of Irrdir varies from 25° to 55°, RR materials can be used primarily to mitigate the UHI effect during the coldest months of the year, while they are ineffective during the other periods because of the sun elevation (Table 12).

The application of RR materials on the horizontal surface should follow the best practices described above for the application on the vertical surface in the Central zone. In the Northern zone the difference in the solar geometry leads to a reduction of the angular interval, and the recommended range is between 35° and 55°. In the Southern zone, the application of RR materials is effective during the whole year (Table 12).

Table 12 Overview of the boundaries of activation of RR ideal materials.

		Vertical surface									**Horizontal surface**								
		Norther Zone			**Central Zone**			**Southern Zone**			**Norther Zone**			**Central Zone**			**Southern Zone**		
		Oulu	Oslo	Copenhagen	Brussels	Milan	Madrid	Valletta	Cairo	Doha	Oulu	Oslo	Copenhagen	Brussels	Milan	Madrid	Valletta	Cairo	Doha
Period of activation	Spring	■	■	■		■	■				■	■	■	■	■	■	■	■	■
	Summer	■	■	■		■	■				■	■	■	■	■	■	■	■	■
	Fall					■	■	■	■	■							■	■	■
	Winter							■	■	■							■	■	■

Angular range of RR activation	25° - 55°	30° - 70°	25° - 55°	35° - 55°	30° - 70°	0° - 90°

6. Conclusions and further developments

The development of RR systems represents a possible step to enable new technologies and strategies to mitigate the UHI effect. This study proposes an inverse approach to define the selective properties of ideal RR materials, which are optimized according to different climatic zones and latitudes, leading to the definition of guidelines about the application of RR systems and their further development. In this work, the magnitude and impact of some phenomena, which are already well known such as the effect of solar geometry on solar energy collected by the envelope, are presented. The solar irradiation analyses, which were conducted on vertical and horizontal surface, confirmed that the application of RR material on a horizontal surface can contribute to reduce the absorption of high amounts of direct solar irradiation through the year which might lead to UHI effects.

An ideal, optimized RR material should not reflect back the totality of the Irrdir, but is expected to select the available direct solar irradiation depending on the season, in order to reduce the need for cooling (and the UHI effect) while still exploiting solar gains in the colder season. The evaluation of the angular distribution of Irrdir carried out in this study allowed the selective properties of an ideal RR material to be investigated. The most relevant properties and practices identified in this paper are highlighted in the list below.

• In the case of a horizontal surface, the application and activation of selective properties of RR materials is efficient in almost all the analysed locations since the solar irradiation in warmer months represents most of the yearly distribution of the solar irradiation;

• In the case of a vertical surface, the performance level is influenced by the solar geometry as shown by the correlation between the seasonal direct contributions and the latitudes of the case study cities. For example, the RR materials applied in locations closer to the Equator in warm season are as not effective as in the cold periods due to the lower sunray angles of Irrdir incident on the vertical plane;

• The selective behaviour of the ideal RR material needs to retro-reflect the solar irradiation incident on the vertical, south-exposed surface within an interval between 25° and 55°, whereas on a horizontal surface the angular range required is even wider – from 30° to 90°.

The next step of the research activity initiated with this study will focus on the development of a model and the execution of simulations for quantifying the advantages of the application of ideal RR materials characterized by a selective behaviour in an urban district, and in particular in some urban canyon configurations. In parallel, a validation of the optical behaviour of the numerical model of the urban canyon with conventional and RR materials will be carried out to verify the robustness of the simulation environment that will be used to assess the impact of RR systems at urban scale.

Acknowledgements

The authors wish to thank the Norwegian University of Science and Technology (Trondheim, Norway), the University of Perugia (Perugia, Italy) and the CIRIAF – Interuniversity Research Center on Pollution and Environment "Mauro Felli" for having supported the collaboration between the two universities in this work, framed by the EU programme for education, training, youth and sport – 'ERASMUS+'. This research was hosted by The Research Centre on Zero Emission Neighbourhoods in Smart Cities (FME ZEN) at NTNU, a centre established with the support from the Research Council of Norway and several partners.

The authors gratefully acknowledge the anonymous reviewers who helped to drastically improve the quality of the paper, and Ellika Taveres-Cachat for her assistance in proofreading the manuscript. However, it goes without saying that any errors in the article are the product of the authors' own doing.

References

Akbari, H. and Touchaei, A. G., 2014. Modeling and labeling heterogeneous directional reflective roofing materials. *Solar Energy Materials and Solar Cells* 124, 192–210. doi: 10.1016/j.solmat.2014.01.036.

Brans, K. I., Engelen, J. M. T., Souffreau, C., De Meester, L., 2018. Urban hot-tubs: Local urbanization has profound effects on average and extreme temperatures in ponds. *Landscape and Urban Planning* 176, 22–29. doi: 10.1016/J.LANDURBPLAN.2018.03.013.

Castellani, B., Morini, E., Anderini, E., Filipponi, M., Rossi, F., 2017. Development and characterization of retro-reflective colored tiles for advanced building skins', *Energy and Buildings* 154, 513–522. doi: 10.1016/j.enbuild.2017.08.078.

Cotana, F., Morini, E., Castellani, B., Nicolini, A., Bonamente, E., Anderini, E., Cotana, F., 2015. Beneficial effects of retroreflective materials in urban canyons: results from seasonal monitoring campaign. *Journal of Physics: Conference Series*, 655(1), paper ID 12012. http://stacks.iop.org/1742-6596/655/i=1/a=012012.

Han, Y., Taylor, J. and Pisello, A. L., 2015. Toward Mitigating Urban Heat Island Effects: Investigating the Thermal-Energy Impact of Bio-Inspired Retro-reflective Building Envelopes in Dense Urban Settings. *Energy and Buildings* 102, 380-389. doi: 10.1016/j.enbuild.2015.05.040.

Hassid, S., Santamouris, M., Papanikolaou, N., Linardi, A., Klitsikas, N., Georgakis, C., Assimakopoulos, D.N., 2000. Effect of the Athens heat island on air conditioning load, *Energy and Buildings* 32, 131-141. doi: 10.1016/S0378-7788(99)00045-6.

Ibrahim, M., Wurtz, E., Biwole, P.H., Achard, P., 2014. Transferring the south solar energy to the north facade through embedded water pipes. *Energy* 78, 834–845. doi: 10.1016/J.ENERGY.2014.10.078.

Ichinose, M., Inoue, T., Nagahama, T., 2017. Effect of retro-reflecting transparent window on anthropogenic urban heat balance. *Energy and Buildings* 157, 157–165. doi: 10.1016/j.enbuild.2017.01.051.

Inoue, T., Shimo, T., Ichinose, M., Takase, K., Nagaham, T., 2017. Improvement of urban thermal environment by wavelength-selective retro-reflective film. *Energy Procedia* 122, 967-972. doi: 10.1016/j.egypro.2017.07.447.

Kottek, M., Grieser, J., Beck, C., Rudolf, B., Rubel, F., 2006. World Map of the Köppen-Geiger climate classification updated. *Meteorologische Zeitschrift* 15, 259-263. doi: 10.1127/0941-2948/2006/0130

Lin, L., Lin, L., Ge, E., Liu, X., Liao, W., Luo, M., 2018. Urbanization effects on heat waves in Fujian Province, Southeast China. *Atmospheric Research* 210, 123–132. doi: 10.1016/J.ATMOSRES.2018.04.011.

Lobaccaro, G., Houlihan Wiberg, A., Ceci, G., Manni, M., Lolli, N., Berardi, U., 2018. Parametric design to minimize the embodied GHG emissions in a ZEB. *Energy and Buildings* 167, 106–123. doi: 10.1016/J.ENBUILD.2018.02.025.

Morini, E., Castellani, B., Presciutti, A., Anderini, E., Filipponi, M., Nicolini, A., Rossi, F., 2017. Experimental Analysis of the Effect of Geometry and Façade Materials on Urban District's Equivalent Albedo. *Sustainability* 9(7), 1245. doi: 10.3390/su9071245.

Morini, E., Castellani, B., Presciutti, A., Filipponi, M., Nicolini, A., Rossi, F., 2017. Optic-energy performance improvement of exterior paints for buildings. *Energy and Buildings* 139, 690–701. doi: 10.1016/j.enbuild.2017.01.060.

Morini, E., Castellani, B., Anderini, E., Presciutti, A., Nicolini, A., Rossi, F., 2018. Optimized retro-reflective tiles for exterior building element. *Sustainable Cities and Society* 37, 146–153. doi: 10.1016/j.scs.2017.11.007.

Nilsen, R. B. and Lu, X. J., 2004. Retroreflection technology. In Proc. SPIE 5616, Optics and Photonics for Counterterrorism and Crime Fighting, pp. 5614–5616. doi: https://doi.org/10.1117/12.577624.

Pantavou, K., TheoharatosG., Mavrakis, A., Santamouris, M., 2011. Evaluating thermal comfort conditions and health responses during an extremely hot summer in Athens. *Building and Environment* 46, 339-344. doi: 10.1016/j.buildenv.2010.07.026.

Qin, Y., Liang, J., Tan, K., Li, F., 2016. A side by side comparison of the cooling effect of building blocks with retro-reflective and diffuse-reflective walls. *Solar Energy* 133, 172-179. doi: 10.1016/j.solener.2016.03.067.

Radhi, H., Sharples, S. and Assem, E., 2015. Model Impact of urban heat islands on the thermal comfort and cooling energy demand of artificial islands — A case study of AMWAJ Islands in Bahrain. *Sustainable Cities and Society* 19, 310-318. doi: 10.1016/j.scs.2015.07.017.

Rossi, F., Pisello, A. L., Nicolini, A., Filipponi, M., Palombo, M.., 2014. Analysis of retro-reflective surfaces for urban heat island mitigation: A new analytical model. *Applied Energy* 114, 621-631. doi: 10.1016/j.apenergy.2013.10.038.

Rossi, F., Castellani, B., Presciutti, A., Morini, E., Filipponi, M., Nicolini, A., Santamouris, M., 2015. Retroreflective façades for urban heat island mitigation: Experimental investigation and energy evaluations. *Applied Energy* 145, 8-20. doi: 10.1016/j.apenergy.2015.01.129.

Rossi, F., Castellani, B., Presciutti, A., Morini, E., Anderini, E., Filipponi, M., Nicolini, A., 2016. Experimental evaluation of urban heat island mitigation potential of retro-reflective pavement in urban canyons. *Energy and Buildings* 126, 340–352. doi: 10.1016/j.enbuild.2016.05.036.

Sakai, H., Emura, K. and Igawa, N., Iyota, H., 2012. Reduction of Reflected Heat of the Sun by Retroreflective Materials. *Journal of Heat Island Institute International* 7(2), 218-221. http://ftp.heat-island.jp/web_journal/HI2009Conf/pdf/30.pdf

Sakai, H. and Iyota, H., 2017. Development of Two New Types of Retroreflective Materials as Countermeasures to Urban Heat Islands. *International Journal of Thermophysics* 38:131. doi: 10.1007/s10765-017-2266-y.

Santamouris, M., 2014. On the energy impact of urban heat island and global warming on buildings. *Energy and Buildings* 82, 100–113. doi: 10.1016/j.enbuild.2014.07.022.

Santamouris, M., Cartalis, C., Synnefa, A., Kolokots, D., 2015. On the impact of urban heat island and global warming on the power demand and electricity consumption of buildings - A review. *Energy and Buildings* 98, 119–124. doi: 10.1016/j.enbuild.2014.09.052.

Santamouris, M. and Kolokotsa, D., 2015. On the impact of urban overheating and extreme climatic conditions on housing, energy, comfort and environmental quality of vulnerable population in Europe. *Energy and Buildings* 98, 125–133. doi: 10.1016/j.enbuild.2014.08.050.

Santamouris, M., Paraponiaris, K. and Mihalakakou, G., 2007. Estimating the ecological footprint of the heat island effect over Athens, Greece. *Climatic Change* 80(3), 265–276. doi: 10.1007/s10584-006-9128-0.

Stathopoulou, E. Mihalakakou, G., Santamouris, M., Bagiorgas, H. S., 2008. On the impact of temperature on tropospheric ozone concentration levels in urban environments. *Journal of Earth System Science* 117(3), pp. 227–236. doi: 10.1007/s12040-008-0027-9.

United Nations (Publisher), 2014. World Urbanization Prospects: The 2014 Revision, Highlights. New York: United Nations. https://esa.un.org/unpd/wup/. ISBN 978-92-1-151517-6

Xu, X., González, J.E., Shen, S., Miao, S., Dou, J., 2018. Impacts of urbanization and air pollution on building energy demands — Beijing case study. *Applied Energy* 225, 98–109. doi: 10.1016/J.APENERGY.2018.04.120.

Yoshida, S., Yumino, S., Uchida, T., Mochida, A., 2015. Effect of windows with heat ray retroreflective film on outdoor thermal environment and building cooling load. *Journal of Heat Island Institute International* 9(2), 67-72.
http://www.heat-island.jp/web_journal/Special_Issue_7JGM/46_yoshida.pdf

Yuan, J., Emura, K., Farnham, C., Sakai, H., 2016. Application of glass beads as retro-reflective facades for urban heat island mitigation: Experimental investigation and simulation analysis. *Building and Environment* 105, 140–152. doi: 10.1016/j.buildenv.2016.05.039.

Yuan, J., Emura, K., Sakai, H., Farnham, C., Lu, S., 2016. Optical analysis of glass bead retro-reflective materials for urban heat island mitigation. *Solar Energy* 132, 203–213. doi: 10.1016/j.solener.2016.03.011.

Yuan, J., Emura, K. and Farnham, C., 2014. A method to measure retro-reflectance and durability of retro-reflective materials for building outer walls. *Journal of Building Physics* 38(6), 500-516. doi: 10.1177/1744259113517208.

Yuan, J., Emura, K. and Farnham, C., 2016. Potential for Application of Retroreflective Materials instead of Highly Reflective Materials for Urban Heat Island Mitigation. *Urban Studies Research* Volume 2016, Article ID 3626294. doi: 10.1155/2016/3626294.

Yuan, J., Farnham, C. and Emura, K., 2015. A study on the accuracy of determining the retro-reflectance of retro-reflective material by heat balance. *Solar Energy* 122, 419–428. doi: 10.1016/j.solener.2015.08.040.

Yuan, J., Farnham, C. and Emura, K., 2015. Development of a retro-reflective material as building coating and evaluation on albedo of urban canyons and building heat loads. *Energy and Buildings* 103, 107–117. doi: 10.1016/j.enbuild.2015.06.055.